

# **HELEX: Heliophysical Explorers: Solar Orbiter and Sentinels**

**Report of the Joint Science and Technology Definition Team (JSTDT)**

PRE-PUBLICATION VERSION

## Contents

<b>HELEX Joint Science and Technology Definition Team .....</b>	<b>3</b>
<b>Executive Summary .....</b>	<b>4</b>
<b>1.0 Introduction .....</b>	<b>6</b>
1.1 Heliophysical Explorers (HELEX): Solar Orbiter and the Inner Heliospheric Sentinels .....	7
<b>2.0 Science Objectives .....</b>	<b>8</b>
2.1 What are the origins of the solar wind streams and the heliospheric magnetic field? .....	9
2.2 What are the sources, acceleration mechanisms, and transport processes of solar energetic particles? .....	13
2.3 How do coronal mass ejections evolve in the inner heliosphere? .....	16
2.4 High-latitude-phase science .....	19
<b>3.0 Measurement Requirements and Science Implementation .....</b>	<b>20</b>
3.1 Measurement Requirements .....	20
3.2 Observational Strategy .....	23
3.3 Supporting Observations .....	25
<b>4.0 Theory and Modeling .....</b>	<b>25</b>
<b>5.0 Mission Design .....</b>	<b>27</b>
Appendix A - Solar Orbiter Science Requirements Document (ESA 2005)	
Appendix B - Solar Sentinels: Report of the Science and Technology Definition Team (NASA 2006)	

## HELEX Joint Science and Technology Definition Team

Robert P. Lin (co-chair)  
*University of California, Berkeley, CA, USA*

Eckart Marsch (co-chair)  
*Max-Planck-Institut für Sonnensystemforschung,  
Lindau, Germany*

Spiro Antiochos  
*Naval Research Laboratory, Washington DC,  
USA*

Thierry Appourchaux  
*Institut d'Astrophysique Spatiale, Orsay, France*

Joseph M. Davila  
*NASA Goddard Space Flight Center, Greenbelt,  
MD, USA*

Silvano Fineschi  
*Osservatorio Astronomico di Torino, Italy*

Alan Gabriel  
*Institut d'Astrophysique Spatiale, Orsay, France*

Jean-François Hochedez  
*Observatoire Royal de Belgique, Brussels,  
Belgium*

Timothy Horbury  
*Imperial College, London, UK*

Glenn Mason  
*The Johns Hopkins University Applied Physics  
Laboratory, Laurel, MD, USA*

Richard Mewaldt  
*California Institute of Technology, Pasadena,  
CA, USA*

Alan Title  
*Lockheed Martin Advanced Technology Center,  
Palo Alto, CA, USA*

Robert Wimmer-Schweingruber  
*Christian-Albrechts-Universität zu Kiel, Germany*

## Ex Officio Members

Madhulika Guhathakurta  
LWS Program Scientist  
*NASA/HQ, Washington DC, USA*

Haydee M. Maldonado  
Sentinels Project Manager  
*NASA Goddard Space Flight Center, Greenbelt,  
MD, USA*

Adam Szabo  
Sentinels Study Scientist  
*NASA Goddard Space Flight Center, Greenbelt,  
MD, USA*

O. C. St. Cyr  
LWS Project Scientist  
*NASA Goddard Space Flight Center, Greenbelt,  
MD, USA*

Hermann Opgenoorth  
Head of Solar System Missions Division  
*ESA-ESTEC, Noordwijk, The Netherlands*

Philippe Kletzkine  
Solar Orbiter Project Manager  
*ESA-ESTEC, Noordwijk, The Netherlands*

Richard Marsden  
Solar Orbiter Study Scientist  
*ESA-ESTEC, Noordwijk, The Netherlands*

William Lewis  
(Technical Writing Support)  
*Southwest Research Institute, San Antonio, TX,  
USA*

## **Heliophysical Explorers (HELEX): Executive Summary**

Heliophysical Explorers (HELEX) brings together and augments the unique capabilities of ESA's Solar Orbiter mission (near-Sun and out-of-ecliptic in-situ plus remote-sensing observations) with those of NASA's Inner Heliospheric Sentinels (in-situ observations from multiple platforms arrayed at varying radial distances and azimuthal locations in the near-ecliptic plane) to investigate, characterize, and understand how the Sun determines the environment of the inner solar system and, more broadly, generates the heliosphere itself. This joint ESA-NASA science program offers a unique opportunity for coordinated, correlative measurements, resulting in a combined observational capability and science return that far outweighs that of either mission alone. Building on the knowledge gained from groundbreaking missions like Helios and Ulysses, and more recently STEREO, HELEX will bring to bear the power of multipoint, in-situ measurements using previously unavailable instrumental capabilities in combination with remote-sensing observations from a new, inner-heliospheric perspective to answer fundamental questions about the Sun-heliosphere linkage. The three overarching questions to be addressed by the HELEX program are:

- What are the origins of the solar wind streams and the heliospheric magnetic field?
- What are the sources, acceleration mechanisms, and transport processes of solar energetic particles?
- How do coronal mass ejections evolve in the inner heliosphere?

To answer these questions, it is essential to make in-situ measurements of the solar wind plasma, fields, waves, and energetic particles close enough to the Sun that they are still relatively unprocessed. It is also necessary to make simultaneous in-situ measurements at multiple locations in order to capture the spatial structure and temporal evolution of the phenomena being observed and to perform imaging and spectroscopic observations of the source regions on the Sun simultaneously with the in-situ measurements.

The mission design that will enable HELEX to accomplish these objectives foresees a launch of Solar Orbiter in 2015, followed two years later by Sentinels. A NASA-provided launch vehicle will place Solar Orbiter into an inner heliospheric orbit that will bring the spacecraft as close to the Sun as  $\sim 0.23$  AU by the end of the transfer phase and, through progressive raising of the inclination employing Venus gravity assist manoeuvres, to heliolatitudes of  $27.5^\circ$  by the end of the nominal mission phase and to  $\sim 34^\circ$  by the end of the extended mission. Four Inner Heliospheric Sentinels spacecraft will be launched together into a heliocentric orbit in the orbital plane of Venus. Three or four Venus gravity assist maneuvers will be

performed over 2.5 to 3 years to bring the four spacecraft into their final orbits, with perihelia at 0.25 AU and aphelia at 0.76 AU.

In addition to formulating the three HELEX science themes, the Joint Science and Technology Definition Team (JSTDT) convened by ESA and NASA recommended significant changes to the Solar Orbiter and Sentinels payloads and operational modes to optimize them for the joint mission. Most importantly, synoptic observations were added to the observational strategy of Solar Orbiter, thereby providing the remote-sensing observations needed to link the multipoint in-situ measurements by Sentinels to features observed on the Sun. Other recommendations by the JSTDT include the addition of a wide-field heliospheric imager to the payload of Solar Orbiter that would allow concurrent remote imaging of the same regions that are being sampled in-situ by one or more of the four Sentinels. Finally, the measurements to be made by Solar Orbiter and the Sentinels were prioritized for the joint mission objectives.

Thus, HELEX will explore the near-Sun environment, determine how the Sun generates the dynamic heliosphere, and elucidate the fundamental plasma physical processes operating near the Sun and their coupling across multiple scales. Moreover, the knowledge gained from HELEX will be both relevant to our understanding of remote astrophysical processes, which are inaccessible to direct measurement, and directly applicable to our efforts to predict and mitigate the effects of space weather.

## 1.0 Introduction

The solar system resides within a region of the interstellar medium in our galaxy that is defined by the outflow of plasma and magnetic fields from the Sun. Within this volume of space, which is known as the heliosphere, the Earth, the other planets, and most other solar system bodies are immersed in a highly dilute medium composed of plasma, neutral gas, dust, solar energetic particles, cosmic rays, electromagnetic radiation, and magnetic fields. A fundamental goal of solar and heliospheric physics is to characterize this medium, in both its quasi-steady and perturbed states, to relate its properties and behavior to the magnetically driven activity of the Sun, and to understand its interactions with the bodies immersed in it and with the interstellar medium beyond. Of particular interest are the sources of the supersonic outflow of plasma known as the solar wind, which carries with it a portion of the Sun's magnetic field, and the eruptive releases of energy, magnetic flux, and matter at the Sun that episodically perturb this more or less steady outflow and accelerate some small fraction of the coronal and solar wind plasma to extremely high energies.

These questions—the sources of the solar wind, the disruption of the Sun's magnetic field in eruptive events, the production of solar energetic particles (SEPs)—have been subject to intensive observational investigation, from both space and the ground, and theoretical study since the early 1960s, when a series of Russian and American spacecraft provided the confirmation of the solar wind's existence and revealed the presence of its fast and slow components. During the ensuing four decades, a flotilla of spacecraft have measured the solar wind and the heliospheric magnetic field (HMF), first in two dimensions, in the plane of the ecliptic, and then, with the launch of Ulysses in 1990, in the third (out-of-ecliptic) dimension as well. In parallel with the characterization of the solar wind through in-situ measurement, imaging and spectroscopy from both ground- and space-based observatories have provided increasingly detailed views of the upper corona, transition region, and photosphere and, through helioseismology, of the Sun's interior as well.

By correlating remote-sensing observations of the Sun's corona and photosphere with in-situ measurements of the plasmas, fields, and energetic particles in the interplanetary medium, we have begun to develop an understanding of how processes on the Sun relate to plasma-physical phenomena within the heliosphere and, indeed, of how the Sun generates the heliosphere itself. Apart from advancing our knowledge of our own space environment, the study of the Sun-heliosphere connection offers insight into other, remote astrophysical systems, such as the astropheres around other stars, that are not subject to direct investigation. Moreover, it has immediate practical application to our ability to forecast space

weather, mitigate its effects on vulnerable spacebased and groundbased systems, and reduce the risk posed by SEP events to astronauts and future human explorers of the Moon and Mars.

Despite the significant advances in our knowledge and understanding of the Sun-heliosphere connection that have occurred over the past four decades, a number of fundamental questions remain to be answered. Our ability to answer those questions has been significantly limited by the fact that, except for the pioneering but relatively primitive observations made by Mariner 10 (1973) and Helios 1 (1974-1986) and Helios 2 (1976-1980), the majority of the in-situ measurements of the solar wind, the HMF, and SEPs have been made at 1 AU or beyond. At these distances from the Sun, however, the solar wind plasma, fields, waves, and SEPs have generally been so substantially modified by various poorly understood and often nonlinear processes as they propagate out from the Sun that the information they contain about their origins and evolution has been largely “washed out” (**Figure 1-1**). *In order to advance beyond the present state of our knowledge and to be able to answer some of the outstanding questions about the solar origins of the heliospheric plasma and energetic particle environment, it is necessary to make in-situ measurements of the solar wind plasma, fields, waves, and SEPs close enough to the Sun that they are still relatively unprocessed.* It is also necessary

- to make simultaneous in-situ measurements at multiple locations in order to capture the spatial structure and temporal evolution of the phenomena being observed;
- to trace the magnetic field from the locations where the in-situ measurements are made back to the source regions on the Sun; and
- to perform imaging and spectroscopic observations of the source regions on the Sun simultaneously with the in-situ measurements.

## **1.1 Heliophysical Explorers (HELEX): Solar Orbiter and the Inner Heliospheric Sentinels**

Two solar-orbiting missions currently in the planning stage have been designed to return to the inner heliosphere. Each will meet some of the measurement requirements outlined above; together, the two missions will satisfy all of them. The European Space Agency’s *Solar Orbiter* is a three-axis stabilized spacecraft equipped with instruments for both in-situ measurements and remote-sensing observations. It will be placed into an elliptical orbit about the Sun with perihelia ranging from 0.23 to 0.38 AU and aphelia from 0.73 to 0.88 AU. After an in-ecliptic phase of perihelion passes where it is nearly corotating with the Sun, Solar Orbiter will use multiple Venus gravity assist maneuvers to move the inclination of its orbit to progressively higher heliolatitudes, reaching  $\sim 34.2^\circ$  by the end of its extended mission. (Details of the Solar Orbiter mission are given in Appendix A, the Solar Orbiter Assessment Phase Final Report.)

NASA's *Inner Heliospheric Sentinels* mission is one of three flight elements of the Living with a Star (LWS) Solar Sentinels program defined in the August 2006 report by the Sentinels Science and Technology Definition Team (Appendix B). (The other two flight elements discussed in the report are a Near-Earth Sentinel which would carry a UV spectroscopic coronagraph and a white-light coronagraph with an FOV out to 60  $R_S$  and a Farside Sentinel equipped with a magnetograph for measurement of the photospheric magnetic field. The remote-sensing capabilities supplied by these two spacecraft will be provided in the merged program by Solar Orbiter.) Inner Heliospheric Sentinels (hereafter "Sentinels") mission will place four spin-stabilized spacecraft into an elliptical heliocentric orbit with perihelia near 0.25 AU and aphelia near 0.75 AU. The orbit will remain within a few degrees of the ecliptic. The four Sentinels will be identically instrumented to make comprehensive in-situ measurements of the inner heliospheric plasma and energetic particle environment as well as to perform x-ray imaging of electron acceleration sites and detect gamma-ray/neutron bursts from ion acceleration associated with flares and other transients.

Each mission possesses a capability that the other lacks but needs in order to achieve the richest possible scientific yield: Solar Orbiter provides the remote-sensing capability that the Sentinels require if their in-situ measurements are to be unambiguously related to structures on the Sun, while the Sentinels—with the Orbiter serving as fifth Sentinel—provide the multipoint perspective needed to resolve the spatial and temporal features of transients and other solar wind structures. The complementarity of the two missions has long been recognized, and at the 2nd Solar Orbiter Workshop held in Athens, Greece, in the fall of 2006 it was announced that Solar Orbiter and Sentinels would be joined in a common program. A Joint Science and Technology Definition Team (JSTDT) was formed in early 2007 and charged to 1) define and prioritize the science goals for the joint program, 2) identify and prioritize the measurements required to achieve those goals, 3) assess the strawman payloads of both missions in light of the measurement requirements and suggest optimizations, and 4) develop an observational/mission implementation strategy to achieve the joint science goals. The following document is the report of the JSTDT, which christened the merged Orbiter/Sentinels program HELEX (HELiophysical EXplorers). It presents the results of intense discussions that took place over the course of seven months during three face-to-face meetings and in numerous telecons.

## **2.0 Science Objectives**

HELEX combines the capabilities of ESA's Solar Orbiter (near-Sun in-situ plus remote-sensing observations from a partially co-rotating platform whose orbital inclination gradually rises from near-ecliptic to heliographic midlatitudes) with those of NASA's Sentinels (in-situ observations from multiple

platforms arrayed at varying radial distances and azimuthal locations in the near-ecliptic plane) to investigate, characterize, and understand the Sun’s influence on the environment of the inner solar system. Such understanding is, of course, also the primary goal each mission individually, whose science objectives are described in the reports prepared by the respective science and mission definition teams (see the appendices). *However, the significant overlap in the timing of the two missions affords a unique opportunity for coordinated, correlative measurements, resulting in a combined observational capability and science return much greater than that of either mission alone.* The Joint Science and Technology Definition Team has therefore identified three overarching science questions as the focus of the HELEX program:

- **What are the origins of the solar wind streams and the heliospheric magnetic field?**
- **What are the sources, acceleration mechanisms, and transport processes of solar energetic particles?**
- **How do coronal mass ejections evolve in the inner heliosphere?**

In the following sections, each of these main questions, broken down into a set of more detailed subquestions, is briefly discussed, along with an overview of the measurement strategy that HELEX will employ to address each subquestion. A more detailed discussion of the measurement requirements that follow from the HELEX science objectives as well as of the observational strategies that the joint program makes possible is given below, in Section 3, “Measurement Requirements and Science Implementation.”

## **2.1 What are the origins of the solar wind streams and the heliospheric magnetic field?**

The overall structure of the heliosphere and the role played by the solar boundary conditions in determining this structure are reasonably well understood. During solar activity minimum, large polar coronal holes emit high-speed streams, while the slow wind flows from the (magnetic) equatorial streamer belt. During solar activity maximum, the well-organized bipolar structure of the wind disappears, with slow and fast wind being emitted at all latitudes (**Figure 2-1**), depending on the distribution of streamers and coronal holes and the strongly tilted magnetic solar current sheet. This global description does not, however, address the fundamental questions regarding the solar origin of the solar wind streams.

**2.1.1 How and where do fast and slow solar wind streams originate?** The detailed magnetic topology and dynamical behavior of the source regions of the solar wind are among the fundamental

questions of solar physics. In the case of the fast solar wind, recent research has confirmed its association with coronal funnels, expanding magnetic field structures rooted in the magnetic network lanes [Tu *et al.*, 2005]. The solar wind starts flowing out of the corona in these funnels at heights between 5 Mm and 20 Mm above the photosphere (**Figure 2-2**). This result was obtained by correlating the magnetic field extrapolated from photospheric magnetograms with Doppler-velocity and radiance maps in different spectral lines, a technique that can be used to study other possible source regions of the fast wind (such as the quiet Sun) in much finer detail than previously possible. Polar plumes and “pseudostreamers” have been proposed as additional sources of the fast wind, although their contribution to the bulk flow is thought to be relatively small [Wang *et al.*, 2007].

Although at solar minimum the slow solar wind is clearly associated with the magnetically closed streamer belt (cf. **Figure 2-1**, left panel), its origins, unlike those of the fast wind, remain largely unclear. Is the slow wind simply a boundary layer flow from the coronal streamers, or does it consist of an ensemble of plasmoids emanating from the streamer tops like “leaves in the wind” (**Figure 2-3**)? Since solar plasma is generally confined in coronal loops and streamers, the release of plasma from closed magnetic structures requires intermittent magnetic reconnection. In several recent papers, Fisk and coworkers (e.g., Fisk and Schwadron [2001]) have emphasized the possible role that reconnection between open flux and closed loops might play on a supergranular scale in producing the solar wind (**Figure 2-4**). According to the proposed scenario, the fast wind and the slow wind both ultimately originate in coronal loops, with the loop properties determining the type of wind. Reconnection causes the loops to open up intermittently, releasing plasma into the corona and providing material and energy to the solar wind streams. Similarly, in their coronal funnel model, Tu *et al.* [2005] propose that the magnetoconvection-driven advection of small loops toward coronal funnels or strong flux tubes and the resulting reconnection of the closed and open structures supplies energy in the form of waves and turbulent flows to the nascent fast solar wind (**Figure 2-2**). If the release of plasma from a reconnecting loop is the major mechanism for the generation of the slow wind, the Lorentz force may play a dominant role in its acceleration, the signature of which will appear quite different from that of plasma acceleration driven by thermal or wave pressure gradients on open field lines.

During solar activity maximum, the slow wind emanates from small coronal holes and from active regions, as demonstrated, for example, by Neugebauer *et al.* [2002], who used a potential-field source-surface model to trace the slow and moderately fast solar wind measured by Ulysses and ACE back to its coronal origins in coronal holes and active regions, and by direct field line tracing using electron measurements (Larson *et al.*, 1997). The wind from these two sources was found to differ in both ionic charge states and structure, with the active region outflow being structured in several substreams as opposed to the more homogeneous flow from the coronal holes. In addition, the slow wind produced

during activity maximum differs from that produced during solar minimum, with the former being more turbulent and having greater helium abundance than the latter.

The combination of high-resolution remote sensing from Solar Orbiter with in-situ measurements from both Sentinels and Solar Orbiter will advance significantly our understanding of the origins of the fast and slow wind. Simultaneous measurements from multiple platforms—including from Solar Orbiter’s near-corotating, quasi-heliosynchronous vantage point—will allow us to determine variations in solar wind properties over a broad range of longitudes and over a wide range of near-solar radial distances. We will compare temporal sequences and compositional and kinetic signatures of processes on the Sun to corresponding plasma properties observed in-situ, allowing unambiguous mapping of solar wind packets to their solar origins. Magnetic connectivity will be determined at multiple points in the inner heliosphere by measuring energetic electrons and the associated x-rays and radio emissions and using these measurements to trace the magnetic field lines directly to the solar source regions. Photospheric magnetograms, together with in-situ magnetic field measurements, will make it possible to reconstruct fully the coronal magnetic field by field extrapolation. EUV imaging and spectroscopy will provide the images and plasma diagnostics needed to characterize the plasma state in the coronal loops, which may erupt and deliver material to what then becomes a solar wind stream in the outer corona, where white-light coronagraphy will provide a large-scale view of the stream configuration, including its boundaries. EUV spectroscopy and imaging will make it possible to detect magnetic reconnection in the transition region and corona—e.g., by the observation of plasma jets or of explosive events as seen in the heavy-ion Doppler motions believed to mark the reconnection-driven plasma outflow. These events appear to be associated with impulsive energetic particle bursts observed near 1 AU. The study of the time evolution of such events, and of their particle and radiation outputs, might reveal whether reconnection is quasi-steady or time-varying, and a comparison with magnetograms will indicate the locations of the reconnection sites with respect to the overall magnetic field structure and topology. Thus, HELEX will provide the data needed to relate the properties of the solar wind observed in situ to their possible solar origins as inferred through remote sensing and identified through the extrapolation of magnetic field and plasma flow inward to the corona. A critical role in establishing this relationship and in interpreting the observations and understanding the underlying physical processes will be played by theoretical modeling and numerical simulations (cf. Section 4).

**2.1.2 What are the solar sources of the heliospheric magnetic field?** As discussed above, magnetic reconnection is expected to play a key role in opening up the magnetic field into the corona, from which the solar wind emanates carrying the field with it. The open magnetic flux carried out into the heliosphere by the solar wind—the heliospheric magnetic field (HMF)—is only a small fraction of the overall magnetic flux on the Sun, which largely closes near the surface in the form of multiple small-scale bipolar

regions having strong local magnetic fields (**Figure 2-5**). Where and how does the HMF originate, and what controls the relative fraction of the open flux? What is the relative fraction of open flux coming from coronal holes, and what is the contribution of active regions, which are often associated with neighboring open flux tubes? The unsigned heliospheric radial magnetic flux (corresponding to a field of 3.5 nT at 1 AU distance) is roughly constant over all latitudes and longitudes and, as measurements by Helios and Ulysses have shown, apparently does not change over several successive solar cycles. In view of the variability of coronal structures on all time scales, why does the magnetic flux observed in the heliosphere not show substantial variability as well?

By establishing the connection between the HMF measured in situ with the coronal and photospheric fields, the combined HELEX measurements will provide key insights into the behavior of the global solar and heliospheric magnetic field and help quantify the flux balance in the inner solar system. Photospheric magnetograms from Solar Orbiter will permit the coronal magnetic field to be determined by field extrapolation, magnetometers on both Solar Orbiter and Sentinels will measure the heliospheric field at multiple points in the inner heliosphere, and x-ray/radio/electron measurements will be used for direct field line tracing. EUV imaging and spectroscopy will be used to determine the overall coronal context as well as to provide the information needed to characterize the plasma state in the coronal loops and open-field regions, which all together may contribute to what become solar wind streams.

### **2.1.3 What is the solar origin of turbulence and structures at all scales in the solar wind?**

Coronal structures and fluctuations at all scales are carried out into interplanetary space by the solar wind and are thus imprinted on the heliosphere. Observations have shown the solar wind to be a highly turbulent and dynamically evolving magnetofluid. The fast solar wind is dominated by large-amplitude Alfvén waves, while the slow wind, as measured beyond 0.3 AU (Helios perihelion), is characterized by more fully developed and strongly compressive turbulence. The Alfvén waves in the fast wind are believed to be generated by foot point motions in the photosphere and magnetic reconnection in the network, but the sources of the turbulence in the slow wind are not well understood.

What are the properties of the MHD turbulence observed in interplanetary space, and what do they tell us about its origin? The “flat” spectral slope of  $-1$  in the observed power spectra of magnetic vector-component fluctuations is generally considered to be a signature of the coronal origin of the fluctuations (**Figure 2-6**). On the other hand, the spectral slope of  $-5/3$ , characteristic of higher frequencies, is typical of fully developed fluid turbulence and indicative of the evolution and local modification of the fluctuations as they are carried outward. Nonlinear plasma dynamics or shear flows between interacting streams are local processes that may strongly enhance the original turbulence. What is the detailed physics of the processes generating those features that seem to develop essentially in interplanetary space? Furthermore, observations of solar wind fluctuations inside 1 AU have been made only in the

ecliptic (e.g., by Helios). While Ulysses has given us a look at turbulence at high latitudes, these observations have been made comparatively far away from the Sun ( $>1.5$  AU), even during the fast latitude scans (cf. **Figure 2-1**). How does solar wind turbulence evolve with latitude inside 1 AU?

In addition to the broad spectrum of waves and turbulence, the solar wind carries myriads of fine structures, such as shocks, discontinuities, convected flux tubes (spaghetti model), and current sheets. What are the coronal sources of such solar wind structures, and how do they evolve? The fine structures visible in coronagraph images extend from the corona into interplanetary space over a wide range of scales from mesoscale to smaller scales (**Figure 2-7**). What are the detailed links between such prominent coronal features as plumes or spicules or streamers and structures of similar angular scale observed in the solar wind?

By combining remote-sensing with multipoint in-situ measurements, HELEX is particularly well-suited to identify the source regions of the fluctuations and fine structures observed in the solar wind. The coordinated Solar Orbiter and Sentinels measurements will give us new insights into the behavior of the global and local turbulence pattern, through multipoint in-situ measurements in particular<sup>1</sup>, and will help us to identify the possible origins of MHD turbulence in the inner solar system. In-situ measurements of fluctuations in the plasma fluid velocity, density, and magnetic field at multiple points in the inner heliosphere can be mapped to the coronal magnetic field determined from photospheric magnetograms, while EUV imaging of the coronal sources of the turbulence will provide the information required to characterize the plasma state in active coronal loops and open-field regions that may contribute to the turbulence.

Understanding the origin and evolution of solar wind fine structures requires measurements inside 1 AU and as close to the Sun as possible, where the structures are still relatively unprocessed and before their features have been washed out. In-situ measurements of the HMF and the solar wind plasma will provide the data needed to characterize the plasma state of the convected structures at multiple points in the inner heliosphere and to determine their latitudinal and longitudinal gradients. The coronal sources of the structures and their angular scale sizes will be determined through imaging at EUV and visible wavelengths, while photospheric magnetograms will be used to determine the synoptic coronal magnetic field.

## **2.2 What are the sources, acceleration mechanisms, and transport processes of solar energetic particles?**

---

<sup>1</sup>Compared to previous missions, the number of possible cross-correlations that HELEX can achieve is improved by an order of magnitude.

Solar energetic particles (SEPs) are accelerated at multiple sites including exploding flare loops, magnetic reconnection sites, and shocks that move from the lower corona to the inner heliosphere. The largest events, which can cause dangerous radiation levels at Earth, may include more than one acceleration site. Release of the energetic particles into interplanetary space may be delayed from their acceleration because of trapping in closed magnetic loops or scattering in turbulence near an accelerating shock. On their way to Earth, the particles may be further scattered by the turbulent heliospheric magnetic field. By the time the energetic particles have reached Earth, the effects of acceleration, release, and transport often thoroughly mix the populations so that their source characteristics remain hidden. Only by going closer to the source can we untangle these effects and understand the fundamental processes responsible for the production of SEPs.

### **2.2.1 What are the sources of energetic particles and how are they accelerated to high energy?**

Solar flare explosions can accelerate particles immediately and may also set off instabilities in magnetic structures in the corona that can launch coronal mass ejections (CMEs). These often drive shocks that can begin to accelerate additional energetic particles minutes after the CME is launched and continue to do so for days in the case of the largest events (**Figure 2-8**). What are the roles and importance of these different processes? By making comprehensive measurements close to the Sun where their signatures are more readily identifiable, we can separate and understand their roles (**Figure 1-1**).

The seed particles energized to become SEPs may start out at or near the energy of the local plasma, whose temperature is a few million degrees Kelvin. However, different acceleration sites contain different particle sources, be they the 20 MK plasma in a flaring loop or the ~1-3 MK plasma of the outer corona and solar wind. The so-called suprathermal particles, whose energies are somewhat higher than the local plasma, form a seed particle pool known to be favored in the acceleration of SEPs, since their higher energy gives them a “head start” over the local plasma population. At Earth orbit, the flux of suprathermals (**Fig. 2-9**) shows much more variability than the bulk plasma density. This may be a key factor in the wide range of particle intensities observed in SEP events. Studying the time-varying composition of the suprathermals in the inner solar system will give us critical insights into what material is actually being accelerated.

The very largest SEP events are associated with fast CMEs. Multiple CMEs occur every day at solar maximum, so it is a mystery why only about one CME per month creates a large SEP event. The measured properties of the CMEs and seed particles at Earth orbit do not resolve this puzzle since the acceleration site is much closer to the Sun (**Figure 2-10**). By studying CME events closer to the energetic particle source in the inner solar system, both the properties of the CME-associated shock and the local seed and energetic particle population can be measured, transforming our ability to understand these large space-weather events.

Another class of SEPs originates in small, short-lived (“impulsive”) activity in the lower corona, releasing bursts of electrons that produce a distinctive radio signature as they move through the corona into interplanetary space. The events are also associated with odd mixtures of elements and isotopes easily distinguished from normal solar material. Although they are not as energetic as shock-associated events, impulsive events occur by the thousands each year during active periods and may provide an important component of the SEP seed population. This class of SEP events is believed to originate in association with jets and narrow CMEs; however, their actual sources are generally too small for detection from Earth, but can be observed from the inner heliosphere.

By traveling close to the Sun with remote-sensing and in-situ measurements, Sentinels and Solar Orbiter will revolutionize our understanding of SEPs. The mixing effects, so dominant at Earth orbit, will be largely removed, making source identification and timing studies accurate enough to distinguish among possible particle acceleration mechanisms. By measuring the CME-associated shock and associated turbulence at several points, a global picture will emerge that will link particle properties to the local variables such as shock strength and geometry (quasi-parallel vs. quasi-perpendicular), magnetic field turbulence and orientation, and seed population. In its out-of-ecliptic mission phase, Solar Orbiter will give us the first-ever 360°-longitude views of CMEs, thus providing critical insights into CME geometry that will help explain the wide range in longitudes covered by SEPs. By having global measurements of CME longitudinal size, we can greatly improve the determination of the total energy of the CME, thereby better quantifying the efficiency of particle acceleration by the shock.

**2.2.2 How are solar energetic particles released from their sources and distributed in space and time?** The radiation dose from a large SEP event is often more closely related to its duration rather than its peak intensity. While particle acceleration and release control the peak intensity, the decay phase is controlled by the properties of the interplanetary medium through combined effects of scattering, convection outward by the solar wind, and energy loss (“adiabatic cooling”) of the particles in the expanding solar wind. The mixing of these processes, and the increasing rate of energy loss closer to the Sun, make it critical to understand these effects in the inner heliosphere so that accurate predictions of SEP event decays can be achieved. Thus, in addition to such factors as the specific acceleration mechanism and the seed-particle source discussed in the previous section, the quality of SEP events is determined by the manner in which the particles are released from the corona and their propagation through the inner heliosphere.

SEPs sometimes reach Earth within minutes of an explosion at the Sun, yet in other cases the arrival may be many hours later. We understand in a general way how this behavior can be caused—namely, by trapping the SEPs in closed magnetic structures, poor magnetic connection to the acceleration region, or delays in accelerating the particles themselves since a shock may move through the corona over a period

of hours. Even the small, impulsive SEPs can show significant delays, with the particle release time delayed compared to the radio signature of the particles at the Sun (**Figure 2-11**). Flares that energize large magnetic loop structures sometimes produce energetic particles that travel down the legs of the loop and collide with the denser solar material at the bottom. These collisions release x-rays,  $\gamma$ -rays, and neutrons whose intensities turn out to be poorly correlated with the intensities observed in interplanetary space. By separating the roles of SEP acceleration on loops vs. shocks, we can better understand the nature and timing of energetic particle injection. However, in order to predict SEPs at Earth for space-weather events, a much more detailed understanding is needed, requiring observations closer to the sources of trapping and acceleration.

SEPs travel to Earth spiraling around the local magnetic field line, which can be quite smooth leading to prompt arrival, or which can be very turbulent due to the presence of shocks and solar wind stream interactions. The properties of the shocks, turbulence, and stream-stream interactions in the inner heliosphere need to be measured so that we can understand their effects on the particles (see **Figure 1-1**). This is where HELEX will revolutionize our understanding of SEP release, propagation, and decay. Multipoint measurements will make it possible to distinguish between point sources for SEPs such as flare loops vs. broad-front sources such as shocks. Because the effects of particle scattering are smaller nearer the Sun, timing information about SEP onset obtained by HELEX in the inner heliosphere (at  $\sim 0.35$  AU) will be 3-5 times better than that derived from measurements at 1 AU. The remote-sensing instruments will identify flare sites and activity against which particle timing signatures can be compared with only minimal propagation and transport effects close to the Sun. Proton-driven waves play an important role in particle transport; measurement of such waves in the inner heliosphere, where they are hypothesized to be  $>5$  times more intense than at 1 AU, will advance our understanding of SEP propagation and enable the development of more realistic transport models. Impulsive SEP electrons can be accurately extrapolated back to the lower corona, providing an excellent test of global models of the coronal magnetic field (see Section 4.0).

## **2.3 How do coronal mass ejections evolve in the inner heliosphere?**

The most energetic manifestations of solar activity and the drivers of the most severe space weather here at Earth are the giant disruptions of the Sun's magnetic field observed as a coronal mass ejection (CME)/eruptive flare event. It is now well accepted that the shocks produced by fast CMEs are the primary source for the SEP storms discussed in the previous section. Knowledge of the properties and behavior of CMEs is also critical for understanding the Sun-heliosphere coupling discussed in Section 2.1. Ulysses has shown that during solar maximum, CMEs dominate the structure and dynamics of the

heliospheric field and plasma at all latitudes. Finally, these major events offer the best opportunity to study fundamental physical processes such as magnetic reconnection and instability—processes that define the discipline of heliophysics and that are important throughout the cosmos. By measuring simultaneously the macro- and microscale properties of CME/eruptive flares near their origin, HELEX will revolutionize our understanding not only of these critically important phenomena but also of the processes underlying a vast range of cosmic activity. With the unique capabilities of HELEX we will be able to answer the following fundamental questions:

- How is the structure of ICMEs related to their origin?
- How does the Sun add and remove magnetic flux from interplanetary space?
- How and when do shocks form near the Sun?

**2.3.1. How is the structure of ICMEs related to their origin?** All current CME models predict that the topology of interplanetary CMEs (ICMEs) is that of a twisted flux rope as a result of the flare reconnection that occurs behind the ejection. This result holds irrespective of the particular mechanism that initiates the ejection or of the initial topology of the erupting field. Observations at 1 AU, however, find that less than half of all ICMEs, even those associated with strong flares, have a flux rope structure. Many ICMEs at 1 AU appear to have a complex magnetic structure with no clearly-defined topology. This conflict between theory and observations is one of the outstanding problems in understanding CMEs; moreover, it is also a critical obstacle to predicting space weather. As is well known, the direction of the interplanetary field at the magnetopause is the most important quantity for determining geoeffectiveness. For most CMEs, however, our models fail completely to capture the variations of their magnetic fields. A related problem is the scarcity of prominence plasma detected in ICMEs. It is widely believed that CMEs are driven by the eruption of highly sheared magnetic field lying at the base of the corona—the so-called filament channel. These channels of sheared field generally (but not always) contain cool plasma observable as a prominence/filament. In fact, prominence material is frequently visible in coronagraph images of CMEs close to the Sun, but prominence plasma is very rarely observed at 1AU (**Figure 2-12**).

At present, it is not known if the disagreements between theory and data and between the solar observations and in situ measurements are due to some fundamental error in the models, propagation effects, or some other, unknown effect. To advance our understanding of the structure of ICMEs and its relation to CMEs at the Sun, we must measure their properties as close to their origin as possible. Furthermore, if we are to unravel the complex topology of ICMEs, we must measure their magnetic and plasma properties at multiple points. HELEX has been designed to deliver exactly the type of data

needed. Solar Orbiter will observe the magnetic field and plasma within and around the eruption and will image the CME as it travels outwards, over the Sentinels spacecraft. These, in turn, will measure the detailed magnetic and plasma properties (including composition) at multiple locations. To illustrate the power of such observations, **Figure 2-13** presents two images from the Heliospheric Imager (HI) on STEREO showing the dislocation of the tail of comet Encke due to the passage of a CME. If we were to replace Encke with one of the Sentinels, or even better, several Sentinels at different locations along the CME front, we would be able to measure, for the first time, both the global and the local structure of a CME near its origin. Such data would revolutionize our understanding of CME structure and evolution.

**2.3.2 How do transients add magnetic flux to and remove it from the heliosphere?** A central objective of solar/heliospheric physics is to understand how the flux that connects the Sun to the heliosphere evolves. This is also one of the most puzzling problems in heliophysics, because there appears to be a contradiction between the observed evolution of the solar and of the heliospheric magnetic fields. Remote-sensing observations of the Sun indicate that coronal magnetic flux opens and closes continuously in response to changes in the photospheric flux distribution and to CMEs. For example, the distribution of coronal holes changes dramatically with the solar cycle, and large transient coronal holes often form and decay as part of a major CME event. The images of the Sun suggest that the heliospheric flux must vary substantially both on the short (hours for transient coronal holes) and long (months for polar holes) time-scales. On the other hand, in-situ measurements in the heliosphere reveal an approximately constant magnetic flux. The in-situ data do show some evidence for the addition of new flux to the heliosphere during CMEs, but rarely for the subtraction, and outside of CMEs there is little evidence for flux addition and essentially none for flux subtraction.

Both the addition and the subtraction of heliospheric flux must occur near the Sun, inside the Alfvén radius ( $\sim 20 R_{\odot}$ ). Because of multiple stream-stream interactions and wave turbulence, direct measurements of the heliospheric flux at 1 AU and beyond are too noisy to allow a precise determination of any flux addition or subtraction. Consequently, the most commonly used method for inferring flux variations is measurement of the electron heat flux, but the interpretation of these measurements is also subject to large uncertainties owing to the possible complex evolution of the field and plasma as it propagates out to 1 AU. Thus, to understand how the interplanetary flux evolves, its variations must be measured as close to the Sun as possible.

By traveling closer to the Sun than ever before, HELEX will deliver the definitive observations that will finally resolve the flux addition/subtraction problem. Sentinels will directly measure the magnetic structure of CMEs close to the Sun and will make electron heat flux and energetic electron field-line tracing measurements to determine the CMEs' connection to the Sun. Furthermore, these measurements will be performed by making a number of separate cuts through a CME, including sampling in radial

distance from the Sun. Remote-sensing measurements from Orbiter, particularly magnetograms and EUV images, will quantify the transient opening and closing of flux on the Sun resulting from the launch of a CME. By linking these two sets of measurements, over a range of solar distances, HELEX will provide critically needed new insights into the variations of heliospheric magnetic flux. While CMEs play a major role in the evolution of heliospheric magnetic flux, HELEX will also study the question of flux addition and subtraction during smaller transient events as well as in the heliospheric current sheet and inslow and fast solar wind streams (Section 2.1.2).

**2.3.3. How and when do shocks form near the Sun?** A comprehensive determination of the properties of shocks near their solar origin is essential if we are to make progress on understanding and predicting SEPs. In spite of decades of observational and theoretical work, the relative importance of shocks versus some other flare-associated mechanism for particle acceleration is still the subject of intense debate. CMEs with apparently similar properties, such as speed and size, can have very different SEP productivity. It is not known whether this is due to the properties of the shock, (quasi-parallel versus quasi-perpendicular), the local environment, or propagation effects. Thus, it is important to understand the formation and evolution of shocks in the corona and through the inner heliosphere. Shocks form when disturbances exceed the local magnetosonic speed (generally, the fast magnetosonic speed). Hence, to understand the formation of shocks near the Sun, we need to determine the spatial distribution and temporal variation of the plasma pressure and the magnitude of the magnetic field within the corona. The kinetic, non-fluid description of shock formation and evolution, however, requires detailed understanding of the microphysics in the corona.

HELEX will use remote sensing (e.g., remote radio observations, off-limb spectroscopy, etc.) to determine the position and speed of shocks over a range of near-solar distances. The goal will be to detect shocks at their earliest formation. At the same time, multipoint in-situ plasma and magnetic field measurements will quantify their micro properties, such as turbulence levels, while measuring the SEPs (cf. Section 2.2). For the first time we will determine how shock properties vary with location along the shock front while the shock is still accelerating particles in the inner solar system. Varying the interspacecraft separations will be critical to the success of this study. By measuring the global and local properties of shocks as near to their origin as possible, HELEX will resolve the question of whether shocks are the only mechanism for SEP production and greatly advance our understanding of how shocks can accelerate particles so effectively. This understanding will be important for interpreting a host of astrophysical observations, and will be vital to any deep-space human exploration program.

## **2.4 High-Latitude-Phase Science**

The out-of-the-ecliptic phase of the Solar Orbiter mission will, for a 2015 launch, begin in 2020, near the end of the nominal Sentinels mission and the beginning of Orbiter's extended mission phase (see Section 5.0 below). Should extended missions be approved for both Solar Orbiter and Sentinels, Orbiter's observations from progressively higher heliolatitudes—reaching over 34°—would add a third dimension to HELEX's multipoint measurement capability and enable the first coordinated investigation of the three-dimensional structure of the inner heliosphere by spacecraft in multiple locations. For example, correlative observations from high and low heliolatitudes would make it possible to study the latitudinal transport of solar energetic particles, which is poorly understood. Coronagraphic imaging from Orbiter's out-of-ecliptic perspective would reveal the longitudinal structure and extent of streamers and CMEs, whose heliospheric manifestations the Sentinels measure in-situ at different locations in the ecliptic. In addition, from near 30° heliolatitude, the Solar Orbiter coronagraph will be able to see over the Sun's pole and also image the far side of the Sun, providing contextual observations for significantly more of the Sentinels orbits than is possible from low latitudes.

### **3.0 Measurement Requirements and Science Implementation**

#### **3.1 Measurement Requirements**

The JSTDT carefully defined a set of measurements required to achieve the three HELEX primary science objectives (**Table 3.1**) and identified an additional set of supporting measurements that could be made if adequate resources should become available. **Table 3-2** shows both the required and supporting measurements in relation to the specific questions subsumed under each of the three major HELEX objectives. The JSTDT reviewed the strawman payloads of Solar Orbiter and Sentinels in light of these requirements and then prioritized the measurements further, classifying them as Baseline, Minimum, and Augmented, with a view to providing a basis on which the candidate payloads could be optimized and harmonized. This exercise was performed separately for Solar Orbiter and Sentinels. The results are given in **Table 3-3** and **Table 3-4**. A set of instruments that satisfies only the Minimum measurement requirements represents the minimum acceptable payload for either mission. Should a payload not be able to meet the Minimum measurements, the overall science return would become questionable.

Solar Orbiter's remote-sensing capabilities were a major focus of the team's deliberations from the very outset of the JSTDT activity. The team recommended that synoptic remote-sensing observations be made at low cadence and low resolution throughout the Orbiter's 150-day orbit, which necessitates a change in Solar Orbiter's original operations strategy (see below, Section 3.2.4). In addition, it became clear early on that the HELEX science objectives required the addition of a wide-field coronagraph or

heliospheric imager to the Orbiter's payload in order to provide images of the extended corona with a field of view large enough to encompass the Sentinels perihelia, thus allowing in-situ measurements by Sentinels to be directly related to the coronal structures observed by Sentinels. Finally, the team noted that the capability to make off-disk spectroscopic measurements of the corona out to  $3 R_S$  above the limb would be desirable because it would make it possible to study shocks responsible for the acceleration of energetic particles subsequently measured in situ.

The JSTDT also evaluated the in-situ capabilities of both missions. The relevant difference between the two missions with respect to their in-situ measurement capabilities is that Solar Orbiter is a 3-axis stabilized spacecraft, while the Sentinels are spinners. Because Orbiter is 3-axis stabilized, multiple detector heads would be required to achieve full three-dimensional coverage, whereas on Sentinels a single side-viewing detector can provide nearly a full-sky field of view as the spacecraft spins. On the other hand, Orbiter's 3-axis stabilization greatly increases the time resolution of which Orbiter's plasma instrumentation is capable, while on Sentinels the temporal resolution is generally limited by the spacecraft spin period ( $\sim 3$  seconds).

In order to free the spacecraft resources needed to add a heliospheric imager or wide-field coronagraph, while at the same time exploiting the synergy with Sentinels, the JSTDT suggests that the following changes be made to the original Solar Orbiter reference payload:

- The number of look directions for the energetic particle and plasma instruments can be reduced (few sensor heads and harness) in recognition of the better alternatives given by the spinning Sentinels.
- The dust instrument can be removed, since dust measurements are not required to address the three key HELEX objectives, neither are they essential for the four original Solar Orbiter goals.
- Measurements in the following categories, while important for the joint mission objectives, need not be made on Solar Orbiter and all Sentinels: x-ray imaging and spectroscopy, gamma-ray detection, and neutron detection. For x-ray imaging and spectroscopy (as for other types of solar imaging) a Sun-pointing instrument on a 3-axis stabilized spacecraft such as Solar Orbiter provides order of magnitude better sensitivity, angular resolution, and temporal resolution, over a comparable instrument on a spinning spacecraft. Thus this capability is included in the Solar Orbiter minimum payload. In the case of neutron and gamma measurements, the JSTDT recommended not to allocate spacecraft resources to dedicated sensors on Solar Orbiter. However, some limited neutron and gamma-ray measurement capabilities could be incorporated in another Solar Orbiter instrument. Alternatively, those measurements would be left for Sentinels.

Solar Orbiter’s payload complement has been further streamlined by eliminating the following instruments included in the High Priority Augmentation category: Neutrals, Coronal Radio Sounding, and Total Solar Irradiance (TSI) (cf. “Solar Orbiter Mission Requirements Document”). Should additional simplification become necessary to fit within the tightly constrained Solar Orbiter payload resource envelope, a relaxation of the measurement requirements from Baseline to Minimum for the remote-sensing suite (in particular, spatial resolution) may be considered.

The JSTDT notes that the Solar Orbiter payload was defined by a Payload Definition Team that included both European and U.S. scientists. It was assumed that state-of-the-art capabilities, whether from the U.S. or Europe, would be available to achieve the Orbiter scientific objectives. Many parts of the prioritized Solar Orbiter payload for HELEX depend on the availability of such expertise. Thus, for the success of HELEX, it is essential that NASA and ESA make it possible for the required expertise in both the U.S. and Europe to be utilized.

**3.1.1 Generic Heliospheric Imager.** As stated above, the JSTDT recommends that a wide-field coronagraph (WFC) or a heliospheric imager (HI) be added to Solar Orbiter’s payload to provide contextual knowledge of the transients whose properties the Sentinels are measuring in situ. A WFC would provide coverage out to 60  $R_s$ . In contrast, as demonstrated by recent results from the Solar Mass Ejection Imager (SMEI) on the USAF Coriolos spacecraft and the HIs on the two STEREO spacecraft, an HI could image steady flow and disturbances throughout much of the IHS orbit (indeed, out to 1 AU and beyond). The Sentinels STDT report describes a WFC that could be flown on Solar Orbiter. Rather than repeat the description given there, we refer the reader to the Sentinels report (Appendix B) and limit the discussion here to a brief description of a generic HI (GHI).

An important difference between a conventional coronagraph and a GHI is that the FOV of the latter need not be Sun-centered. Both SMEI and the STEREO HI’s look away from the Sun and are sometimes called “side-lookers.” SMEI can sweep out the entire sky once per orbit. The STEREO HI FOVs are centered on the ecliptic but extend to just beyond 1 AU.

Coronagraphs generally make measurements at small angles near the Sun, and the scattering efficiency peaks for material in the plane-of-the-sky. To describe the challenges of observing at large elongations from the Sun, the concept of a “Thomson surface” [Vourlidas and Howard, 2006] has been developed. The Thomson surface concept takes into account that the location of maximum scattering efficiency favors the front side of the disk, and that it moves closer to the observer as the elongation grows. Because the Solar Orbiter and Sentinels orbits are elliptical, this effect should be considered and optimized to match scientific goals.

Both SMEI and STEREO HI have broad bandpasses to enhance their ability to gather photons. However, it is clear that additional science may be obtained by isolating portions of the visible spectrum

using filters (as was done for the LASCO externally-occulted coronagraphs on SOHO). Those instruments, as well as the coronagraphs on STEREO, also included polarization filters to address specific scientific goals.

One metric defining the ability to see faint features either close to the Sun or far away is the “stray light rejection” of an instrument. For the low corona, typical values of this parameter are  $10^{-6}$ , measured in units of solar brightness. To observe the middle corona, an externally-occulted, Sun-pointed coronagraph can achieve values of  $10^{-9}$ . For GHI, values of  $10^{-14}$  or greater will be required.

The temporal cadence of GHI is governed by several factors, bounded by saturation from bright objects (planets, stars, comets) and radiation exposure on the short end, up to the need to build up sufficient signal to detect faint features on the long end. As an example, STEREO HI accomplishes this by summing a series of short (~1 minute duration) exposures, removing cosmic rays onboard, and downlinking a composite summed image every 60-120 minutes. Resulting image cadence can be measured in “hours” because of the vast distances traversed by features moving through such a large FOV.

Spatial resolution is probably not a driving requirement for GHI because of the large scale features being tracked and the large FOV. With a nominal temporal resolution of one hour, even an extremely fast CME (3200 km/s used as an example in the Sentinels STDT Report) would travel a bit more than  $16 R_S$  (~0.08 AU). A more typical CME speed of 400 km/s therefore covers less than 0.01 AU in an hour, so an appropriate pixel size for GHI will likely be measured in fractions of a degree.

A final consideration is the overlap of GHI field of view with that of other sensors. The SOHO LASCO and EIT instruments were designed as a “nested” set of fields of view, overlapping a small amount between each component. This approach is also used in the design of the STEREO SECCHI suite, where images of the Sun in EUV overlap the inner coronagraph (COR1), which overlap the outer coronagraph (COR2), and so on through the two HI sensors. This design enhances the tracking of features between instruments that have different spatial resolutions and temporal cadences.

### **3.2 Observational Strategy**

The JSTDT determined that continuous low-cadence synoptic remote-sensing observations as well as continuous in-situ measurements by Solar Orbiter are critical to maximize the scientific return of the HELEX program. The requirement for continuous synoptic remote-sensing observations necessitates modifications of the Solar Orbiter observational plan, which originally envisioned operation of the high-bandwidth remote-sensing instruments only for three 10-day “campaign” intervals during a 150-day orbit centered on the high-latitude and closest-approach points. The required modifications, however, are

modest because only low-cadence and low-resolution remote-sensing observations are needed throughout the whole orbit to develop a synoptic picture of the state of the Sun and the inner heliosphere. While significant operational constraints exist that curtail the significant expansion of the total data volume telemetered back from Solar Orbiter, preliminary ESA technical studies show that the existing Solar Orbiter communication subsystem can accommodate most of the identified synoptic observations without impacting the original Solar Orbiter mission objectives, although at times with considerable (3-16 months) data latency.

While continuous synoptic remote-sensing observations are clearly preferred, the JSTDT has identified three particularly favorable orbital configurations with the Sentinels spacecraft when concurrent Solar Orbiter remote sensing observations and Sentinels in-situ measurements are absolutely critical for program success. These configurations are: Quadrature, Conjunction, and Farside.

**Quadrature.** The JSTDT has defined quadrature as the orbital configuration in which one of the Sentinels spacecraft is located in a region from which light scattered from heliospheric structures (e.g., ICMEs) can reach Solar Orbiter with high efficiency. Near the Sun, the spacecraft will be close to true quadrature, with the Sentinel in the plane of the sky. Farther out in the inner heliosphere, quadrature occurs when one of the Sentinels is near the Thompson sphere (see the preceding section). Quadrature configuration is ideal for tracking the radial evolution of ICMEs and shocks and represents one of the revolutionary aspects of the joint HELEX program—namely, the imaging of the regions that are concurrently being sampled by in-situ instrumentation. Thus, in quadrature configuration, wide-FOV coronal imaging from Solar Orbiter with concurrent in-situ fields and particles measurements from Sentinels, possibly combined with Solar Orbiter off-disk spectroscopy, will be particularly important.

**Conjunction.** A second scientifically useful configuration will occur when Solar Orbiter and Sentinels are in conjunction – that is, when any one of the Sentinel spacecraft is within 30° of the Sun-Solar Orbiter line. This configuration will make it possible to correlate plasma diagnostic measurements of the lower corona obtained by dynamic EUV spectroscopy with the same plasma parameters measured in-situ by Sentinels, thus allowing the connection of coronal to heliospheric processes to be determined.

**Farside.** Finally, while the JSTDT assumes that Earth-based or near-Earth assets will provide near-continuous photospheric magnetic field and full-disk EUV imaging of the Sun (cf. Section 3.3), these observations will by definition cover only half the solar surface at any given time. Thus, whenever Solar Orbiter observes the far side of the Sun, it will significantly enhance our ability to determine the context of the Sentinels in-situ observations along their entire orbit and will improve the accuracy of global heliospheric models that will be used to interpret these measurements (cf. Section 4). Low-resolution scalar magnetography and full-disk EUV imaging would be of particular importance in this configuration.

In addition to the above-mentioned relative configurations, during which the Solar Orbiter remote sensing observations will be correlated with the Sentinels in-situ measurements, in-situ measurements by all five spacecraft when they are spaced relative to one another over a significant radial, longitudinal or latitudinal extent will be particularly useful in determining the size, structure and evolution of solar wind structures and in establishing energetic particle beam widths and diffusion patterns. The orbits of the individual Sentinels were designed to maximize the relative motions of the spacecraft and will require continuous in-situ observations from both Solar Orbiter and the Sentinels spacecraft to exploit this capability. Both the Solar Orbiter and Sentinels operational plans fully accommodate continuous in-situ measurements and telemetering of the data acquired. .

### **3.3 Supporting Observations**

Observations from both ground-based radio and optical telescopes and from other spacecraft will be available to support the HELEX program. Groundbased telescopes will provide valuable contextual information both about the structure and dynamics of the corona and about the properties of the solar wind and HMF in the inner heliosphere. In addition to telescopes already in operation in the U.S. and other countries, three advanced telescopes that can contribute significantly to HELEX are expected to come on line during the next decade: the Frequency-Agile Solar Radiotelescope, the Mileura Widefield Array-Low Frequency Demonstrator, and the Advanced Technology Solar Telescope.

Several solar/heliospheric spacecraft missions may be operating during at least the first phase of the HELEX program. The Solar Dynamics Orbiter (SDO), scheduled for launch in 2008, will begin its five-year extended mission in 2013 and will still be operating when Solar Orbiter launches in 2015. A more modest Solar Probe than the one described in the 2005 Solar Probe report is currently being studied. Should “Solar Probe Lite” prove feasible, it may be launched around the same time as Orbiter and would sample the near-Sun region well inside the perihelia of HELEX spacecraft. An additional potential source of supporting data is the Chinese National Space Agency’s KuaFu-A, which would be stationed at L1 and equipped with both remote-sensing and in-situ instruments. Finally, it is conceivable that STEREO, launched in August 2006 with only a planned two-year mission, and the Japanese Hinode mission, launched in October 2006, could still be operational after Solar Orbiter is launched and would be able to provide remote-sensing and in-situ (STEREO) observations in support of HELEX, at least during the program’s early phase.

### **4.0 Theory and Modeling**

Underlying the HELEX science objectives is one of the most challenging problems in all physics: the complex coupling of physical processes across spatial and temporal scales. Microscopic physical processes lead to the formation of macroscopic solar wind streams, kinetic processes combine with large-scale ones (e.g., to accelerate particles), and CME evolution is determined by its micro-and macroscopic interaction with the ambient corona and solar wind. HELEX’s instrumentation and observational strategies are innovatively designed to attack the problem of cross-scale coupling, from the global MHD scales of the Sun’s corona to the local kinetic scales of wave and particle distributions in the heliosphere. But observations alone will not be sufficient. HELEX will be able to measure a significant fraction of the relevant physical scales and at various locations. However, theory and modeling are certainly needed to provide the interpretive framework and also required to elucidate the multiscale connections among the coronal and heliospheric phenomena observed by HELEX. They are thus critical for the HELEX science program to succeed.

A critical motivation for HELEX science is that our understanding of both global and local processes has advanced considerably in recent years. Several large-scale programs are under way in Europe and in the US to develop global MHD models that encompass the whole corona-heliosphere system. At the same time, there have been broad advances in theories for basic mechanisms such as particle acceleration and collisionless reconnection, due in part to NASA’s LWS TR&T program. We expect that the theories and models will greatly increase in sophistication during the next five to ten years, and that HELEX will play a key role in testing and refining the powerful new models. For example, data-driven 3D MHD models of the initiation and development of CMEs are now being developed and should be in a production state by the time HELEX delivers data. By testing these models as close to the CME source as possible, HELEX will deliver breakthrough advances in our understanding and in our ability to predict space weather.

Although substantial progress is expected in understanding the physics at global and local scales, the capability of our theories and models to address the key problem of cross-scale coupling is still relatively primitive and will likely to remain so without a dedicated HELEX theory and modeling program. At the heart of each of the three main science objectives discussed in Section 2 lies a question on cross-scale coupling:

- How do the small-scale processes responsible for heating and accelerating coronal plasma couple with the large-scale magnetic field to produce the observed heliosphere? (Objective 2.1)
- How do the energetic particles accelerated by a shock influence the shock’s evolution and structure? (Objective 2.2)
- How does the global magnetic topology couple with local dissipation processes to produce the fast magnetic reconnection required for flares and CMEs? (Objective 2.3)

To be able to attack these questions with the HELEX measurements, we must start immediately to develop a new generation of theories and models that include cross-scale coupling self-consistently. Given the nature of the problem, the development of useful cross-scale coupling models is a daunting task, but by marshaling the talent and resources of the full international science community, great progress can be made in time for HELEX. SOHO clearly demonstrated that international hardware partnerships have enormous benefit for all partners and can result in impressive advances in space instrumentation. The HELEX program is designed to take full advantage of international hardware partnerships and would benefit by forming similar international partnerships in theory and modeling as well.

Consequently, the JSTDT recommends that international theory and modeling teams (ITMs) be set up as part of the HELEX science program to attack each of the three cross-scale coupling questions above. NASA, ESA, the participating European nations, and the European Research Council should investigate procedures for organizing and selecting these teams as soon as possible and for supporting them during the mission development phase. The HELEX hardware program is bold and innovative, but if the program is to achieve its full science potential, a similarly creative approach to theory and modeling is essential.

## **5.0 Mission Design**

The JSTDT began the HELEX study under the assumption that three Sentinels and Solar Orbiter (replacing the fourth Sentinel) would be launched together on an Atlas EELV. Although a study conducted at NASA/GSFC demonstrated the technical feasibility of this approach, it had become clear by the time of the second JSTDT meeting that the proposed common launch faced considerable challenges in terms of both available resources and schedule. Thus it was jointly decided by NASA and ESA that Solar Orbiter and the Sentinels would be launched separately, with NASA providing the launch vehicle for Solar Orbiter as well as contributing to the Orbiter payload.

According to the current plan, Solar Orbiter will be launched first, followed two or three years later by Sentinels. Solar Orbiter will be placed into a low- $C_3$  inner heliospheric orbit that will require two Earth encounter gravity assist maneuvers and up to seven Venus gravity assist maneuvers to reduce the perihelion distance and to change the inclination of the orbital plane. The Orbiter's reference trajectory will bring the spacecraft as close to the Sun as  $\sim 0.22$  AU by the end of the transfer phase and, through progressive raising of the inclination, to heliolatitudes of  $27.5^\circ$  by the end of the nominal mission phase and to  $\sim 34^\circ$  by the end of the extended mission (**Figure 5-1**). The Solar Orbiter is currently planned to be

launched not later than May 2015, with its nominal mission lasting ~6.2 years but with spacecraft consumables and radiation-sensitive units sized for a ~10-year mission.

The four Sentinels spacecraft will be launched together into a heliocentric orbit in the orbital plane of Venus, i.e., with a 3°-inclination relative to the solar ecliptic plane. Three or four Venus gravity assist maneuvers will be performed over 2.5 to 3 years to bring the four spacecraft into their final orbits, with perihelia at 0.25 AU and aphelia at 0.76 AU.

The earliest programmatically feasible launch opportunity for Sentinels occurs in March 2017, with an August 2018 launch as a backup. A launch on 29 March 2017 with a nominal launch inclination (DLA) of 14.47° requires only modest launch energy ( $C_3 = 22.09 \text{ km}^2/\text{s}^2$ ) and will allow the spacecraft to perform nonresonant encounters with Venus, resulting in final orbits illustrated in **Figure 5-2**. Two Sentinels will be in the same orbit (as indicated by the red line in Figure 5-2) but will be phase-shifted by about 45°; the other two spacecraft will be in orbits whose semi-major axes are significantly rotated relatively to each other and to that of the orbit of the first two Sentinels. The four Sentinels will thus be separated by varying distances both radially and azimuthally, enabling them to study both longitudinal and radial gradients and to determine the extent of large-scale transient structures in the solar wind.

Two dates in 2018 were identified as backup launch opportunities should a 2017 launch not be possible. Neither is as favorable as the 2017 opportunity, however. The first backup launch opportunity would, like the 2017 launch, use nonresonant Venus encounters to place the Sentinels into final orbits similar to those shown in **Figure 5-2** but would require significantly more launch energy ( $C_3 > 30 \text{ km}^2/\text{s}^2$ ). The second launch opportunity, which occurs on 14 August 2018, requires launch energy ( $C_3 = 21.79 \text{ km}^2/\text{s}^2$ ) comparable to that needed for a 2017 launch but would limit the Venus flybys to resonant encounters, thus narrowing the range of final orbital configurations that could be achieved.

The JSTDT investigated the possibility of flying only three Sentinels, with the already orbiting Solar Orbiter replacing the fourth Sentinel in order to achieve the desired multipoint coverage for in-situ observations. Unfortunately, the intervals between possible Sentinels launch opportunities are too large to allow substantial overlap between the low-latitude portion of the Solar Orbiter mission and the Sentinels mission. Even with a 2017 launch, the first Sentinel will not reach 0.5 AU until 14 July 2018, only 88 days before Solar Orbiter enters its first higher-inclination orbit (red segment in **Figure 5-1**), and Sentinels will not reach their final orbits till well over a year later. Helios 1 and 2 observations demonstrated that latitudinal variations in solar wind structures are much more rapid than longitudinal ones; thus corresponding structures could not be positively identified when the two spacecraft were more than 1°-2° apart in latitude. Solar Orbiter's first higher-inclination orbit will be 10° above that of Sentinels and will increase to over 30° in time. Thus, while Solar Orbiter will provide crucial

measurements from the 3rd dimension, it cannot be substituted for one of the Sentinels spacecraft and the original 4-spacecraft configuration described in the Sentinels STDT report is still required.

The Sentinels prime mission is planned to last three years. However, the Sentinels are designed so that they require virtually no consumables, and almost all of the subsystems are dual string. The Sentinels spacecraft can thus reasonably be expected to operate for the entire duration of the extended Solar Orbiter mission, allowing at least ~6 years of coordinated observations by the two missions. With correlated observations by Solar Orbiter at progressively higher heliolatitudes and by Sentinels in the ecliptic, the extended operation of both missions would provide a unique three-dimensional perspective on the structure and evolution of the inner heliosphere around the activity peak of Solar Cycle 25 (~2022) (**Table 5-1**).

## 6.0 References

- Fisk, L.A., and N.A Schwadron, The behavior of the open magnetic field of the Sun, *Astrophys. J.*, **560**, 425, 2001.
- Fisk, L.A., N.A Schwadron, and T.H. Zurbuchen, Acceleration of the fast solar wind by the emergence of new magnetic flux, *J. Geophys. Res.*, **104**, 19765, 1999.
- Horbury, T.S., and B.T. Tsurutani, Ulysses measurements of waves, turbulence and discontinuities, in: *The Heliosphere near Solar Minimum. The Ulysses Perspective*, eds. A. Balogh, R.G. Marsden, and E.J. Smith, p. 167, Springer, London, 2001.
- Larson, D.E., et al., Using energetic electrons to probe the topology of the October 18-20, 1995 magnetic cloud, *Adv. Space. Res.*, **20**, 655, 1997
- Mason, G.M. et al., Energetic particles accelerated by shocks in the heliosphere: What is the source material? in: *The Physics of Collisionless Shocks: 4th Ann. Int. Astrophys. Conf.*, eds. G. Li, G.P. Zank, and C.T. Russell, AIP Conference Proceedings 781, p. 219, AIP Publishing Services, Melville, NY, 2005
- McComas, D.J., et al., The three-dimensional solar wind around solar maximum, *Geophys. Res. Lett.*, **30**, 24-1, doi: 10.1029/2003GL017136, 2003
- Neugebauer, M., et al., Sources of the solar wind at solar activity minimum, *J. Geophys. Res.*, **107**, SSH13-1, doi: 10.1029/2001JA000306, 2002
- Sheeley, N.R., Jr., et al., Measurements of flow speeds in the corona between 2 and 30  $R_s$ , *Astrophys. J.*, **484**, 472, 1997
- Tu, C.-Y., et al., Solar wind origin in coronal funnels, *Science*, **308**, 519, 2005

- Vourlidas, A., and R.A. Howard, The proper treatment of coronal mass ejection brightness: A new methodology and implications for observations, **642**, 1216, 2006
- Wang, Y.-M., N.R. Sheeley, Jr., and N.B. Rich, Coronal pseudostreamers, *Astrophys. J.*, **658**, 1340, 2007
- Wibberenz, G., and H.V. Cane, Multi-spacecraft observations of solar flare particles in the inner heliosphere, *Astrophys. J.*, **650**, 1199, 2006
- Wiegelmann, T. and S.K. Solanki, Why are coronal holes indistinguishable from the quiet Sun in transition region radiation? in: *Proceedings of the SOHO 15 Workshop: Coronal Heating. 6-9 September 2004, St. Andrews, Scotland, UK*, eds. R.W. Walsh et al., ESA SP-575, p. 35, European Space Agency, Paris, 2004

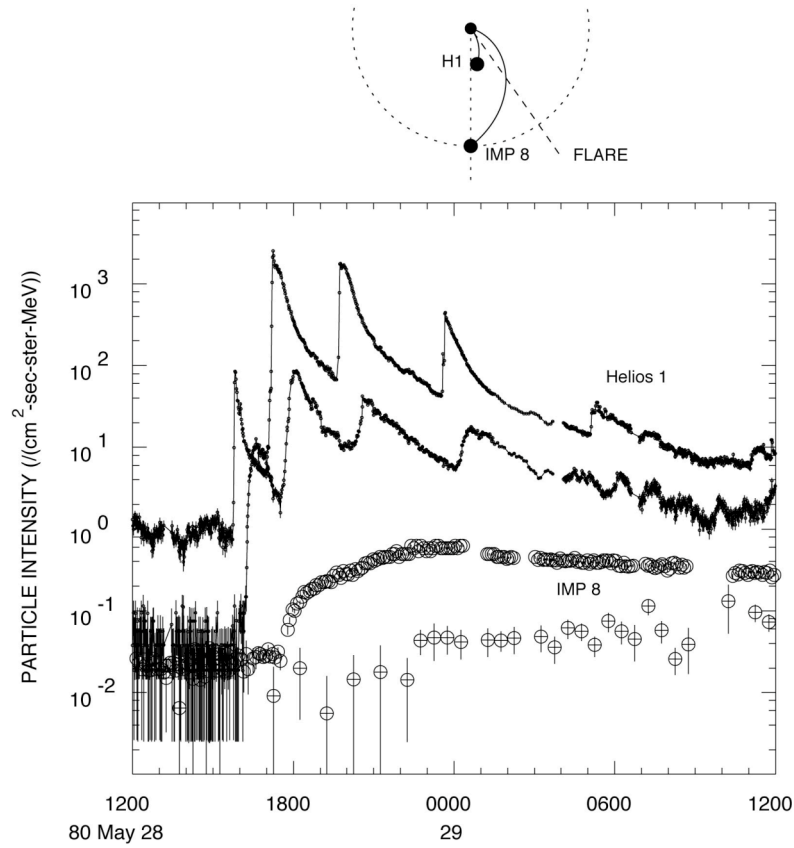


**Figure 1-1.** Electron and alpha particle time profiles recorded by Helios-1 at 0.3 AU and by IMP-8 at 1.0 AU during a series of impulsive particle events on 1980 May 28. Whereas Helios-1 observed multiple injections, no such structures can be resolved in the intensity-time profile at 1 AU. If both spacecraft were observing the same events (and this is not certain), then this plot vividly illustrates both the effects of radial and longitudinal transport inside 1 AU and the need for observations as close to the Sun as possible [Wibberenz and Cane, 2006].

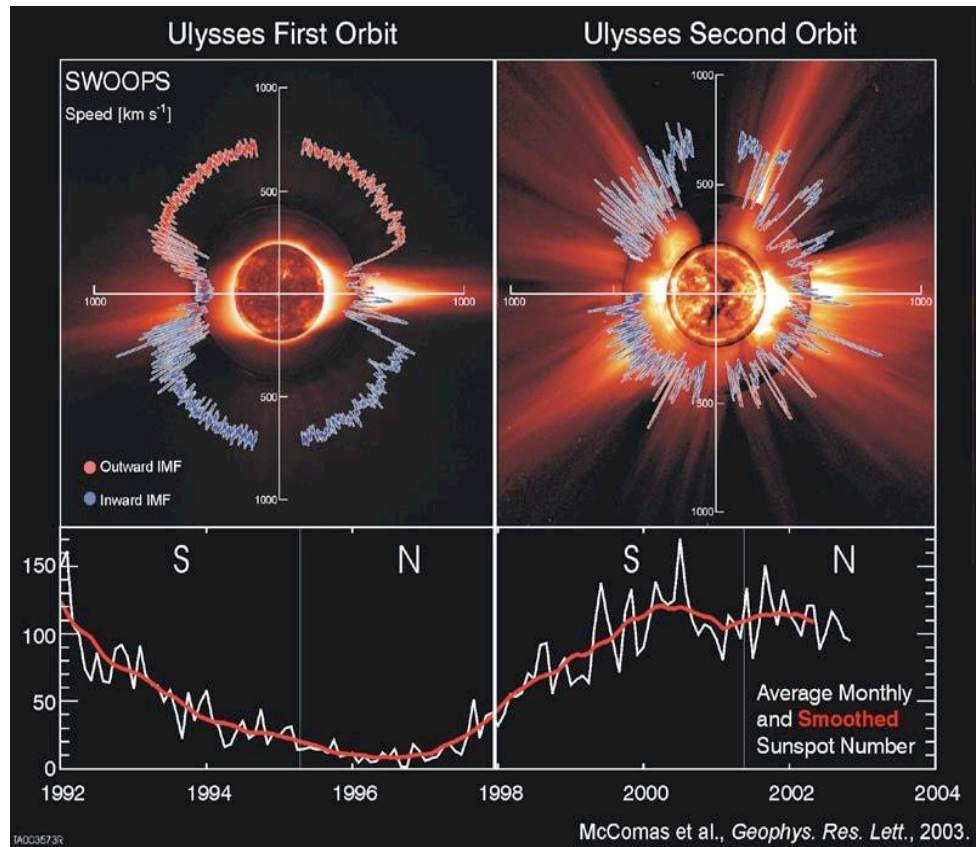


**Figure 2-1** Solar wind velocity data from the SWOOPS instrument on board Ulysses, superposed on images showing the structure of the corona at solar minimum (left) and near solar maximum (right). The sunspot number (average and smoothed) is plotted in the bottom panel. These images clearly show the evolution of the corona and of the associated velocity structure of the solar wind with changing solar activity [McComas *et al.*, 2003].

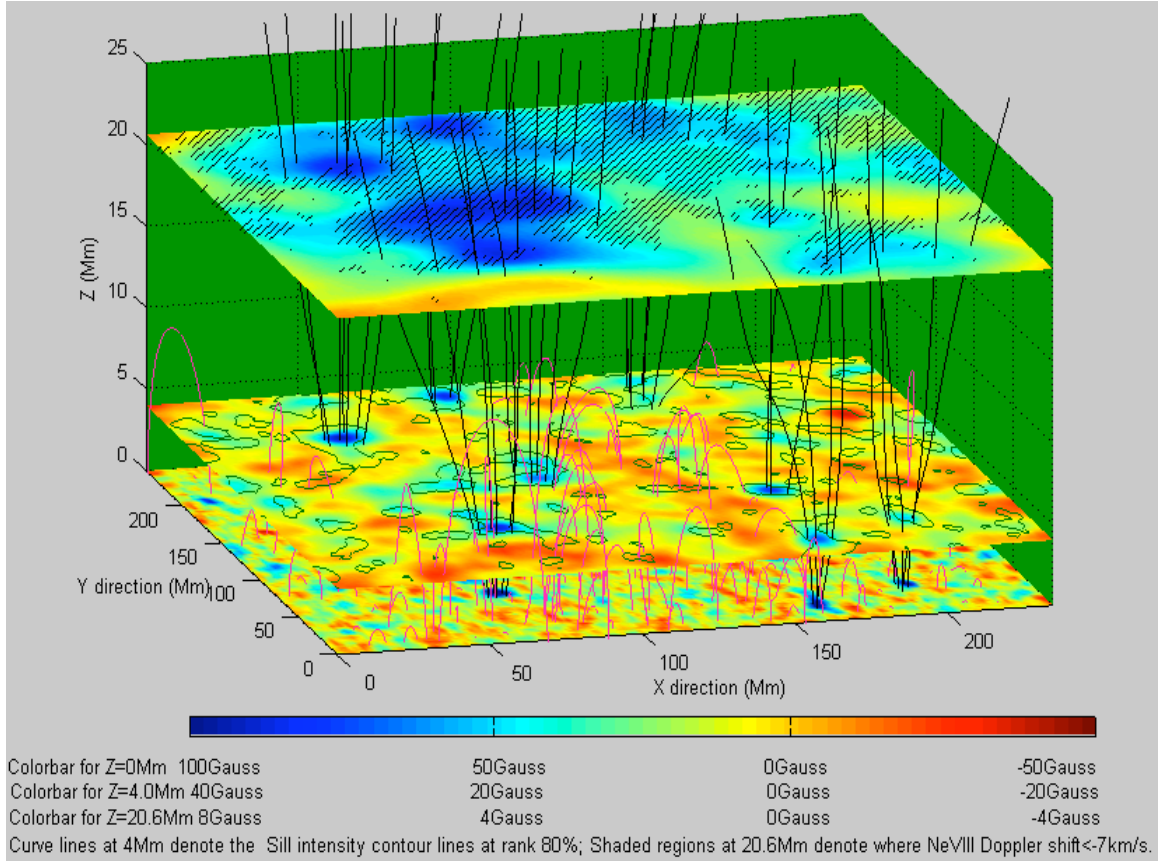


**Figure 2-2** Magnetic field structures in the 3-D solar atmosphere. The black solid curves illustrate open and the red curves closed field lines. Because the magnetic field strength decreases with increasing height ( $Z$ ) in the corona, the scales on the color bars differ for different  $Z$ . In the plane inserted at 4 Mm, we compare the Si II radiance with the extrapolated  $B_z$ . The contours delineate the 80% level of the Si II radiance. In the plane inserted at 20.6 Mm, we compare the Ne VIII Doppler shifts smaller than  $-7$  km/s with the extrapolated  $B_z$ . The shaded areas indicate where the  $\text{Ne}^{7+}$  outflow speed is larger than 7 km/s [Tu et al., 2005].

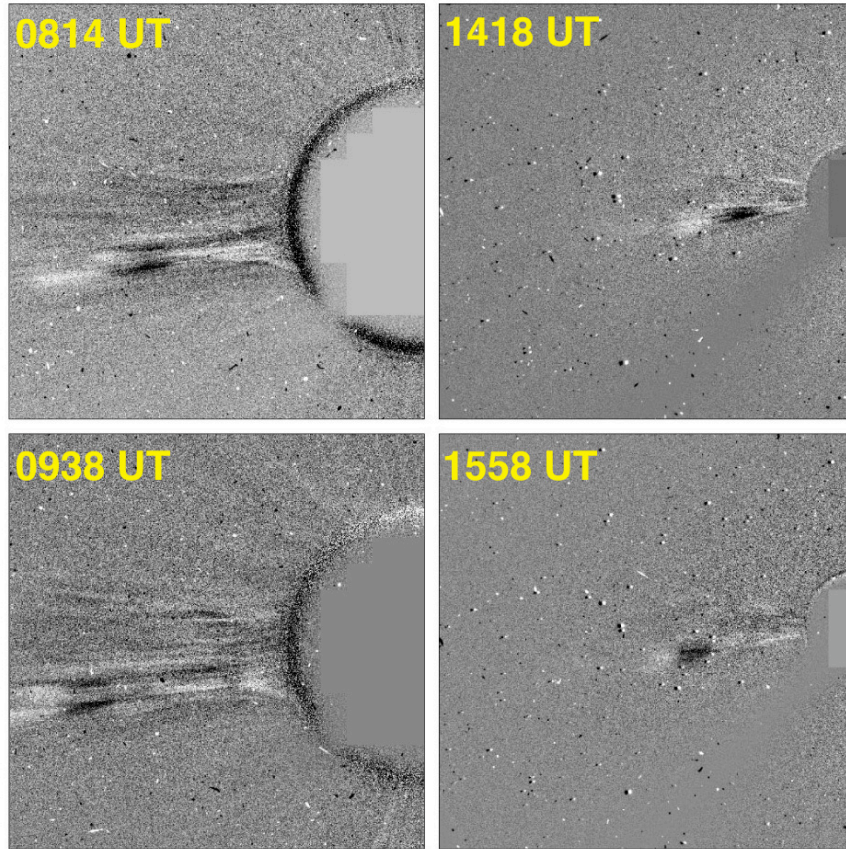


**Figure 2-3.** Recent differenced solar white-light images demonstrated that there is considerable structure inside streamers (like the blobs in this image). However, these structures are completely washed out by 1 AU. A combination of near-Sun in-situ observations providing compositional markers with concurrent solar remote imaging will allow the tracing of the narrow slow solar wind streams to their origination sites [Sheeley *et al.*, 1997].

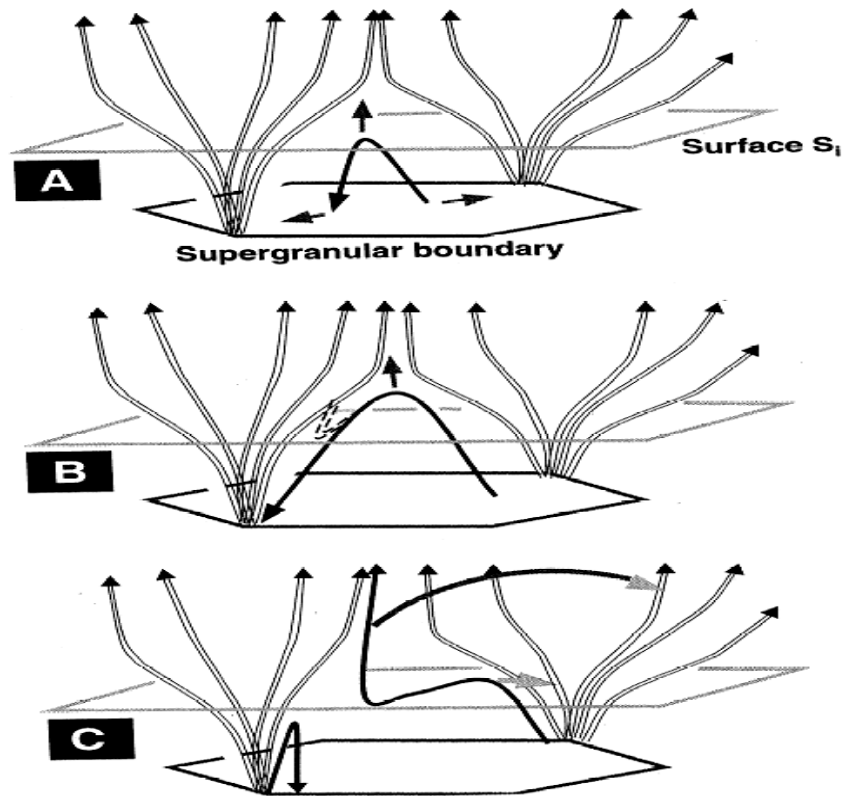


**Figure 2-4** An illustration of the expected behavior of emerging magnetic loops in the photosphere. In (A) a new loop (shown in black) emerges in the center of a supergranule. In (B) the ends of the loop migrate to the boundaries of the supergranule where there are concentrations of magnetic flux (shown in white); only field lines which open into the corona are shown. The end of the loop with polarity opposite to that of the flux concentration reconnects with a field line that opens into the corona. In (C) the new open field line is transported laterally to be reoriented over the other side of the loop [Fisk *et al.*, 1999].

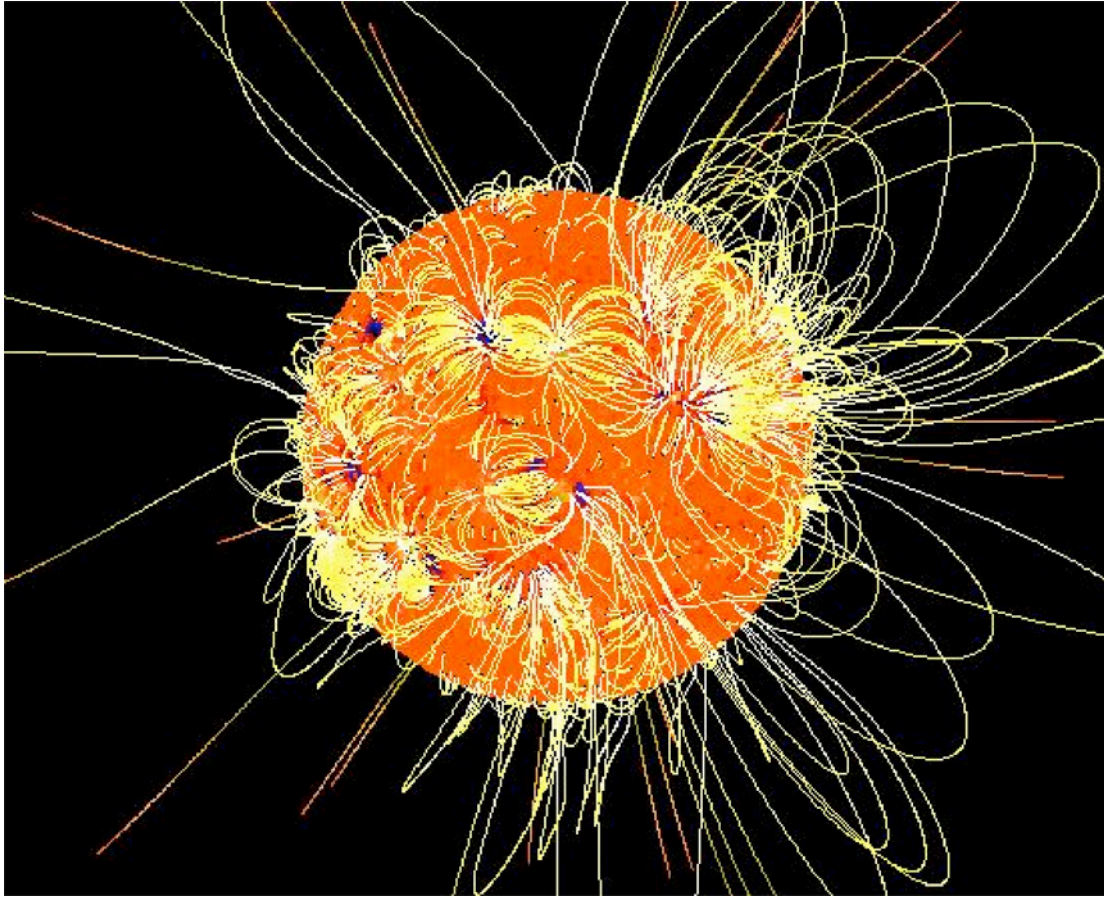


**Figure 2-5** Illustration of the complex solar magnetic field. Shown are many coronal magnetic field lines as obtained by a force-free-field extrapolation from photospheric magnetograms. The closed loops mostly correspond to bipolar active regions, or also may bridge widely separated regions of opposite field polarity, whereas the open lines indicate coronal magnetic fields that are open to the heliosphere. The corresponding magnetic flux is frozen into, and thus carried away, by solar wind streams [*Wiegmann and Solanki, 2004*]

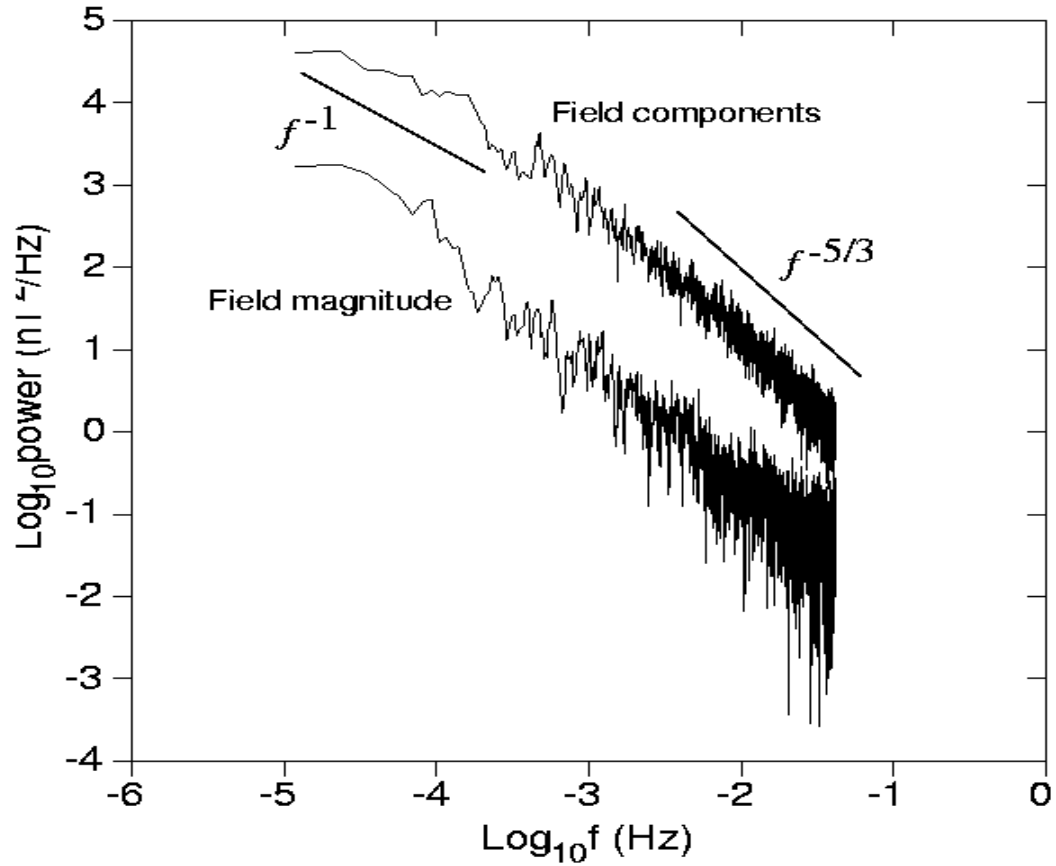


**Figure 2-6** Power spectra of the total component (from the trace of the spectral density matrix) and the magnitude of the magnetic field according to Ulysses measurements made at 1.4 AU and latitude of  $45^\circ$  in the polar heliosphere. Note the two characteristic spectral domains with a slope of  $-1$  (perhaps the solar source spectrum) and of  $-5/3$  indicating developed interplanetary turbulence. The compressive fluctuations are much less intense than the incompressible Alfvén waves [Horbury and Tsurutani, 2001].

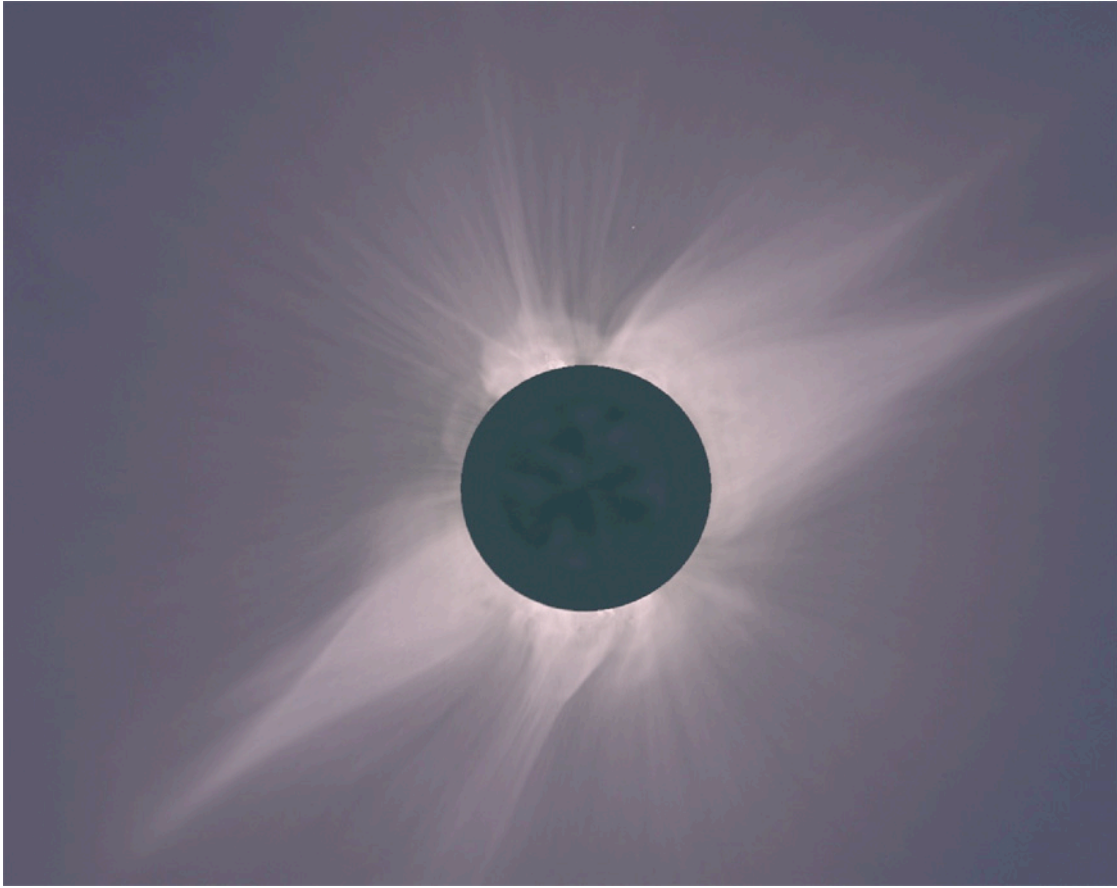


**Figure 2-7.** Eclipse image of the Sun, showing fine-scale coronal structure as well as large helmet streamers.

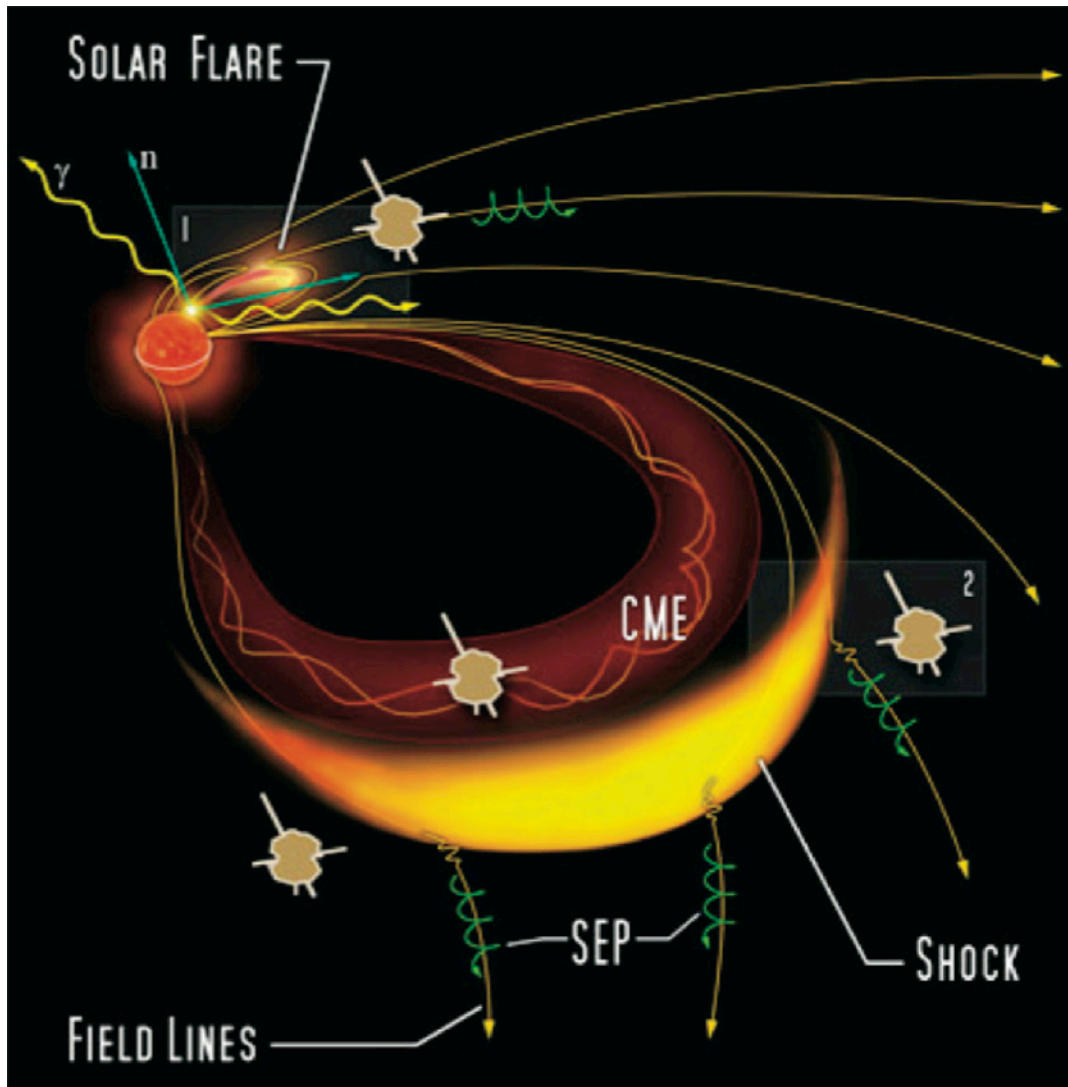


**Figure 2-8** The relative importance of acceleration processes due to flares and CME-driven shocks cannot be determined at 1 AU due to particles mixing. Simultaneous in-situ observations of magnetic field lines connecting back to flare sites and to shock fronts driven by ICMEs—together with concurrent remote imaging of flares, wide field-of-view coronagraphy of CMEs and spectroscopic identification of the CME-driven shocks from Solar Orbiter—are required to determine the relative importance of the associated acceleration processes.

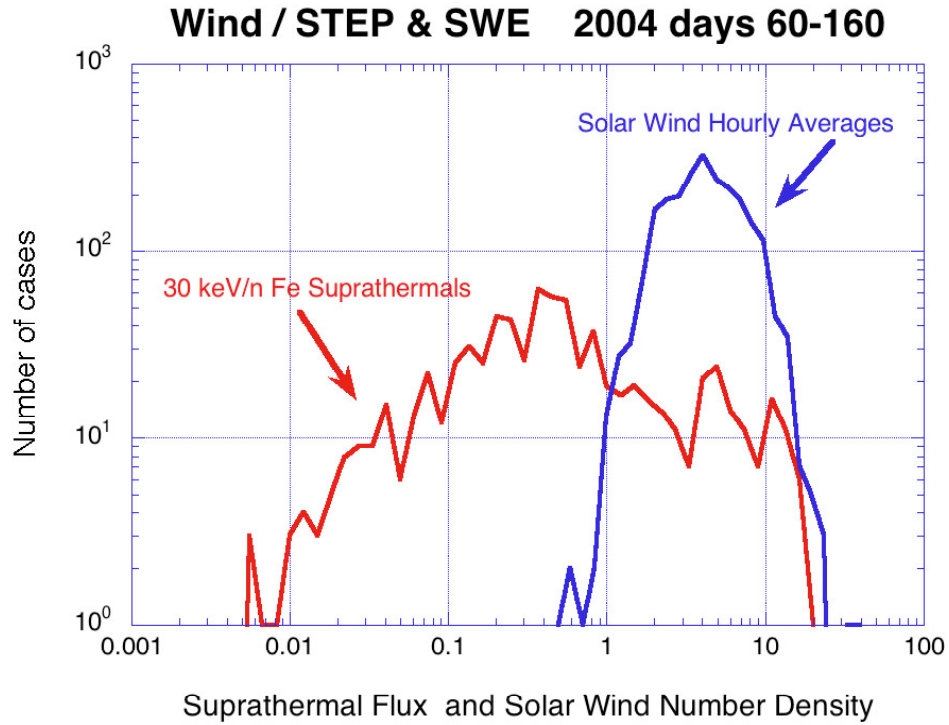
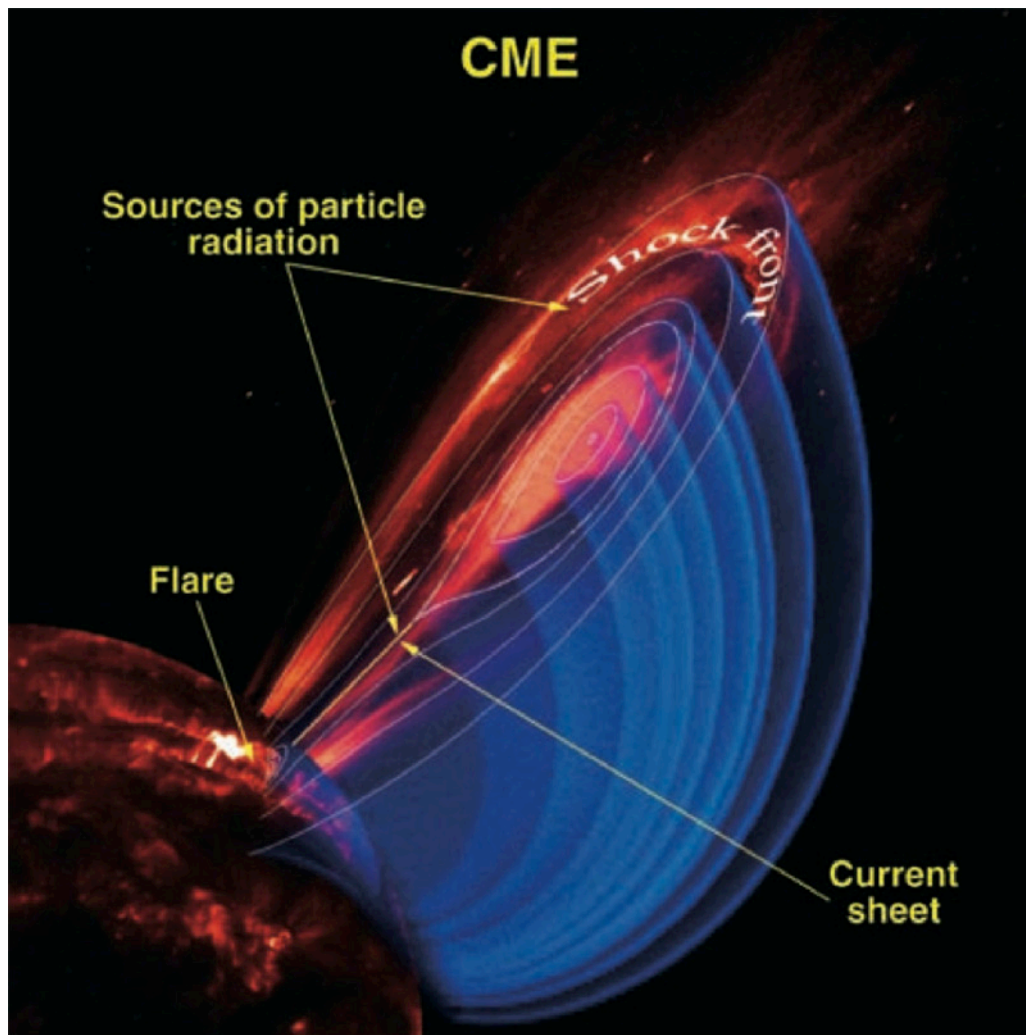


**Figure 2-9** Histograms showing the variation of suprathermal Fe nuclei at Earth orbit compared to the variation of the solar wind density during the same period. While the bulk density varies by only a factor of 10, the suprathermal intensities span a factor of 1000. The large spread in the intensities of suprathermals, which are believed to be an important seed population for large SEP events, may contribute to the observed very large event-to-event variation in SEP intensities [Mason *et al.*, 2005].



06-02357-98

**Figure 2-10** Energetic particles may arise from multiple locations in a complex solar eruption. Each location will have different properties, but due to mixing on the way to Earth these differences cannot be untangled at 1 AU for most cases.

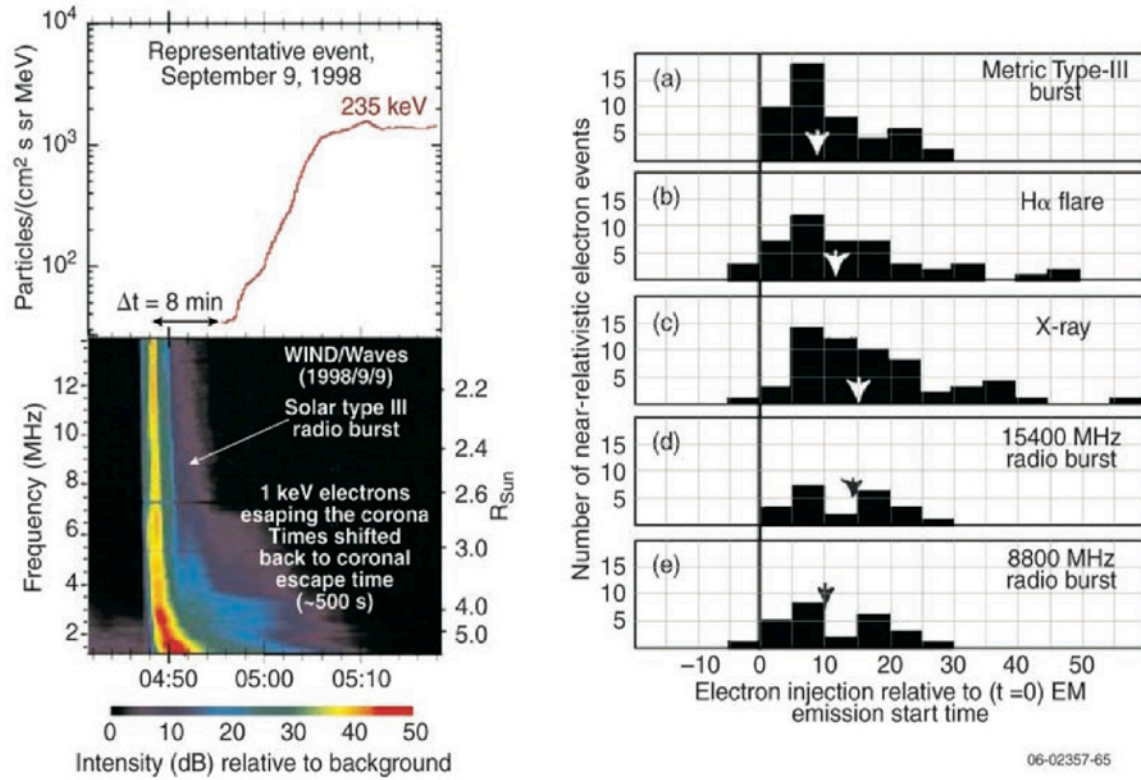


**Figure 2-11** Systematic delays between electromagnetic emissions and interplanetary near-relativistic electrons. The left panel shows a representative event in which the onset of >200 keV electrons is delayed with respect to the start of type III radio emission by ~8 min. Are these delays due to the acceleration process, or are they controlled by the particle escape onto interplanetary magnetic field lines?

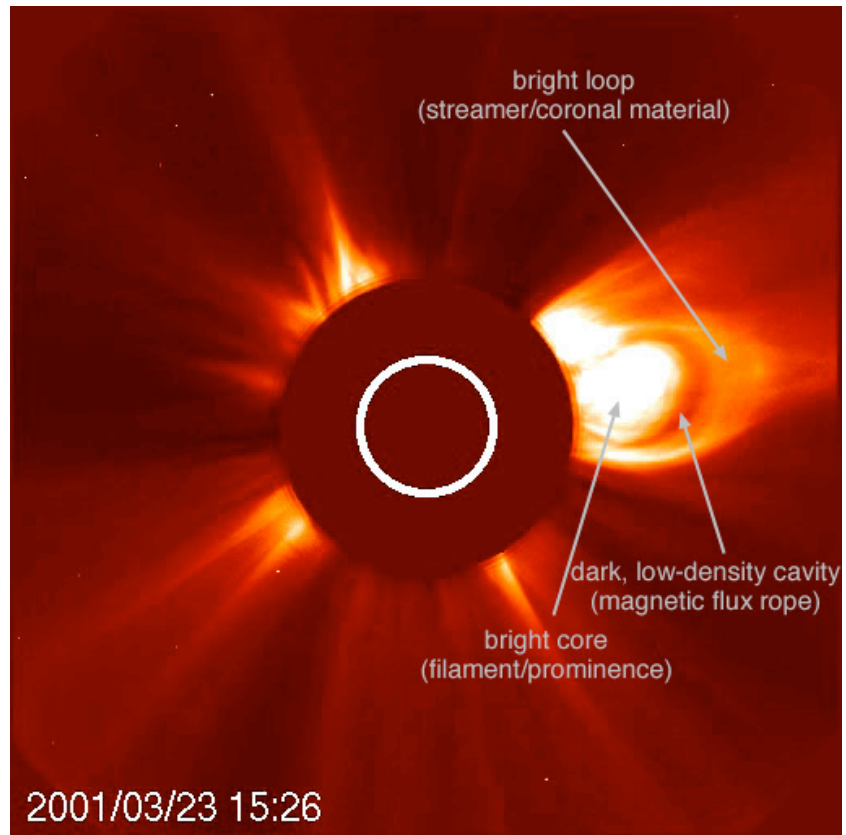


**Figure 2-12** LASCO C2 image showing the classic three-part structure of a CME.

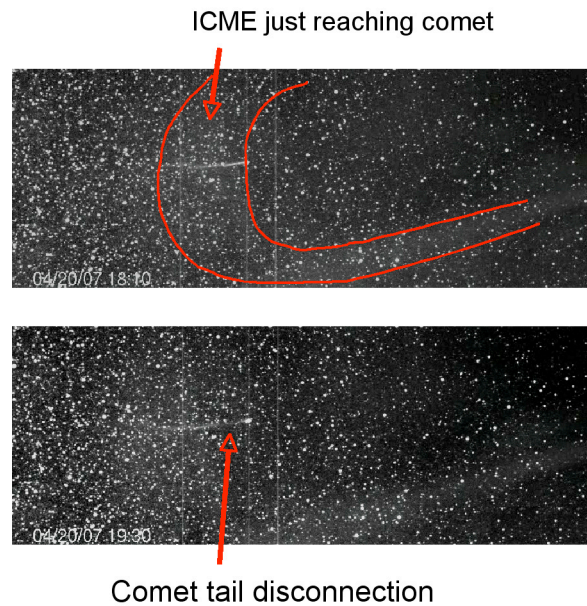


**Figure 2-13** Two images from the Heliospheric Imager on STEREO showing the dislocation of the tail of Comet Encke as the result of the passage of an ICME.

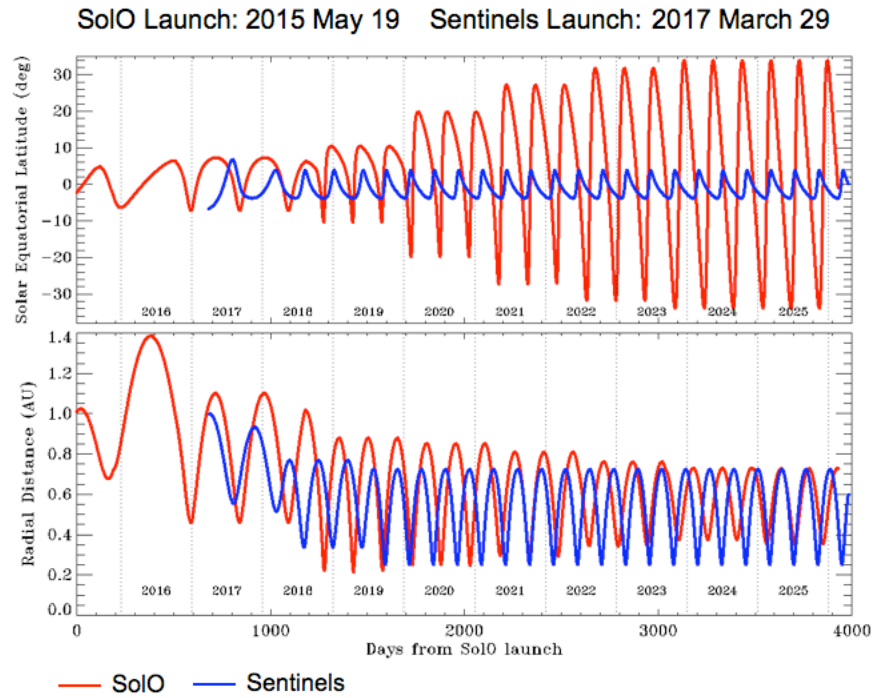


**Figure 5-1** Key orbital features of the Solar Orbiter (in red) and Sentinels (in blue) versus days from launch (of Solar Orbiter in 2015). The top panel shows the solar equatorial latitudes in degrees, and the bottom panel gives the spacecraft radial distances from the Sun in AU. Note that for their whole nominal mission the Sentinels will be in the ecliptic plane together with Solar Orbiter, while in their extended mission phase they become increasingly separated in latitude from, Solar Orbiter, a mission design feature that will permit the study of three-dimensional aspects of the inner heliosphere.

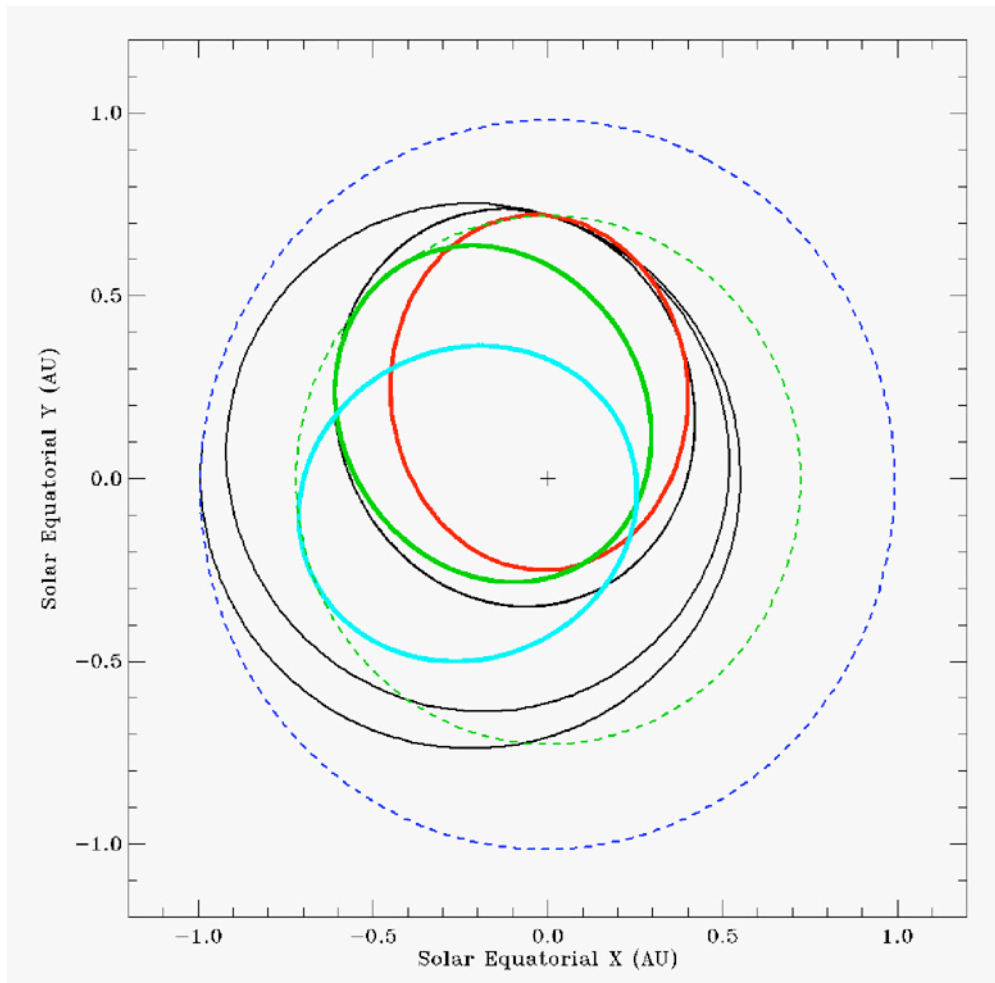


**Figure 5-2** Sentinels final orbits for a 29 March 2017 launch.

<b>Table 3.1</b> Measurements required to achieve the HELEX science objectives			
<b>2.1 Origin of the Solar Wind and HMF</b>			
<b>Energetic Particles</b>	<b>Solar Wind</b>	<b>Fields</b>	<b>Remote Sensing</b>
	Suprathermal electrons Solar wind ions Solar wind electrons (S) Solar wind composition	DC B fields AC B fields Plasma waves (O)	Photospheric fields EUV spectroscopy EUV imaging Near-Sun coronagraphy Wide-angle coronagraphy X-ray imaging
<b>2.2 Sources of Energetic Particles</b>			
<b>Energetic Particles</b>	<b>Solar Wind</b>	<b>Fields</b>	<b>Remote Sensing</b>
Energetic particles EP composition EP charge states	Suprathermal electrons Solar wind ions Solar wind electrons Solar wind composition*	DC B fields AC B fields Remote radio waves (O + 1 S) Plasma waves (O)	EUV imaging Near-Sun coronagraphy Wide-angle coronagraphy X-ray imaging Gamma-ray** Neutron**
<b>2.3 Transients</b>			
<b>Energetic Particles</b>	<b>Solar Wind</b>	<b>Fields</b>	<b>Remote Sensing</b>
Energetic particles EP composition	Suprathermal electrons Solar wind ions Solar wind electrons Solar wind composition	DC B fields Remote radio waves	Photospheric fields EUV imaging Near-Sun coronagraphy Wide-angle coronagraphy X-ray imaging**

\*for suprathermal tail measurements \*\*required on only 1 spacecraft (O) = Orbiter only (S) = Sentinels only

Table 3-2. HELEX measurement prioritization

		Inner Heliospheric Measurements (Sonic point < X < 0.5 AU)																				Coronal Measurements (0 to 60 Rs)																	
		Energetic Particles		Energetic Particle Composition		Energetic Particle Charge State		Suprathermal Electrons		Solar Wind Ions		Solar Wind Electrons		Solar Wind Composition		DC Vector Magnetic Fields		AC Magnetic Fields		Local Plasma Waves		Remote Radio Waves		Photospheric Magnetic Fields		EUV Spectroscopy		EUV Imaging		Near-Sun Coronagraphy		Wide FOV Coronagraphy or HI		X-Ray Imaging		Gamma-Ray Detection		Neutrons	
Obj.	Question	Orb	Sent	Orb	Sent	Orb	Sent	Orb	Sent	Orb	Sent	Orb	Sent	Orb	Sent	Orb	Sent	Orb	Sent	Orb	Sent	Orb	Sent	Orb	Sent	Orb	Sent	Orb	Sent	Orb	Sent	Orb	Sent	Orb	Sent	Orb	Sent		
2.1 What are the origins of the solar wind streams and the heliospheric magnetic field?	2.1.1 Where does the slow and fast solar wind come from?	S	S	S	S			S	S	R	R	S	R	R	R	R	R			R	S	S	S	R		R		R		R		S		R	S				
	2.1.2 What are the solar sources of the HMF?	S	S	S	S	S	S	R	R	R	R					R	R							R			R		R				R	S					
	2.1.3 What is the solar origin of turbulence and structures at all scales in the solar wind?	S	S	S	S						R	R	S	S	S	S	R	R	R	R	R	R	S	S	R		R		R		R								
2.2 What are the sources of energetic particles?	2.2.1 What are the sources of energetic particles and how are they accelerated to high energy?	R	R	R	R	S	R	R	R	R	R	R	R	R	R	R	R	S	S	S	S	R	1st: R 2nd: S	S		S		R		R		R		R	R	1st: R 2nd: S		1st: R 2nd: S	
	2.2.2 How are solar energetic particles released from their sources and distributed in space and time?	R	R	R	R	S	R	R	R	R	R	S	S			R	R	R	R	R	R	S	S	S			S		R		R		S	S					
2.3 How do coronal mass ejections evolve in the inner solar system?	2.3.1 How is the structure of ICMEs related to their origin?							R	R	R	R	S	R	R	R	R	R					S	R	R		S		R		R		R			1st: R 2nd: S				
	2.3.2 How do transients add magnetic flux to and remove it from the heliosphere?	S	S	S	S	S	S	R	R	R	R	S	S	R	R	R	R					S	R	R		S		R		R		R			1st: R 2nd: S				
	2.3.3 How and when do shocks form near the Sun?	R	R	R	R	S	S	S	S	R	R	R	R	S	S	R	R	S	S	S	S	S	R	S		S		R		R		S							

R: Required; S: Supportive Measurement; blank: not needed

Note: With respect to Question 2.2.1, the working group was divided as to whether EUV imaging should be considered required or supportive.

Table 3-3. Prioritized Solar Orbiter Measurements			
Objectives	Minimum Measurements	Baseline Measurements	Augmented Measurements
<b>Energetic Electrons</b>	Energy range: ~2 keV to ~1 MeV, energy resolution: $\Delta E/E \sim 0.2$ , angular resolution 30° over 60° FOV as close to Sun as possible; geometry factor $> \sim 0.1\text{-}1\text{ cm}^2\text{sr}$ ; time resolution 10 s at $< 0.5\text{ AU}$ , 1 min $> 0.5\text{ AU}$	Same as minimum; Burst mode TBD	Baseline plus FOV in anti-Sun direction and full 0-180° pitch-angle coverage
<b>Energetic Protons</b>	Energy range: 0.05 to 100 MeV; energy resolution: $\Delta E/E \sim 0.2$ ; two angular sectors from 0-90° as close to the Sun as possible up to 10 MeV; geometry factor $> \sim 0.1\text{-}1\text{ cm}^2\text{sr}$ ; time resolution 20 s below 10 MeV at $< 0.5\text{ AU}$ , 1 min $> 0.5\text{ AU}$	Minimum plus energy range: 0.005 to $> 100\text{ MeV}$ ; Burst mode TBD	Baseline plus full 0-180° pitch-angle coverage
<b>Energetic Heavy Ions</b>	He – Fe, energy range: 0.02 – 30 MeV/nucleon (species dependent) Composition: separate $^3\text{He}$ , $^4\text{He}$ , C, N,O and Fe as a minimum; energy resolution: $\Delta E/E \sim 0.2$ ; two look directions; geometry factor $> \sim 0.1\text{-}1\text{ cm}^2\text{sr}$ ; time resolution 30 s $< 0.5\text{ AU}$ , 1min $> 0.5\text{ AU}$	Minimum plus energy range to 100 MeV/nucleon (species dependent); Burst mode TBD	Baseline plus additional look directions; full 0-180° pitch-angle coverage
<b>Solar Wind Ions</b>	Simple 1-dim energy spectra (0.2 – 20 keV/q, 5% resolution) of protons and alphas at low time resolution (1 minute), solar wind velocity, density and temperature	Detailed 3-dim velocity distribution functions at 1 s time-resolution; FOV: $\pm 45^\circ$ to Sun, $\pm 15^\circ$ north/south, angular resolution of $2^\circ$	Burst mode at 0.1s time resolution or better for protons for 1 dim
<b>Solar Wind Electrons</b>	Core electron density and temperature, electron strahl over at least $2^\circ$ solid angle; 1 minute	3-dim velocity distribution functions (about 5 -5000 eV, 10% energy resolution); FOV at least $2^\circ$ solid angle, ideally $\pm 180^\circ$ to Sun, $\pm 45^\circ$ north/south, angular resolution $10^\circ$ , core-halo electron pitch-angle distributions with strahl population; 10s resolution	Burst mode: 0.1s distributions to study wave-particle interactions
<b>Solar Wind Composition</b>	Selected heavy ions (C, N, O and Fe) for abundances and charge states; 10 minutes at 0.25AU	Many heavy ion 1-dim energy spectra (0.5 – 60 keV/q, 5% energy resolution); FOV= $\pm 25^\circ$ ; cadence: 1 min at 0.3AU	Temperature anisotropy and differential velocity vector
<b>Local Magnetic Fields and Waves</b>	<b>DC Vector Magnetic Fields:</b> $\pm 1000\text{ nT}$ , 1 minute time resolution; 1nT absolute precision	<b>DC Vector Magnetic Fields:</b> $\pm 1000\text{ nT}$ , 0.5nT absolute precision; 0-20 Hz <b>AC Magnetic Fields:</b> 10Hz – 10kHz; waveform capture	<b>DC Vector Magnetic Fields:</b> Burst mode to 100Hz for shock waves <b>AC Magnetic Fields:</b> 1Hz lowest frequency; enhanced burst mode capture
<b>Local Plasma Waves</b>	Thermal noise electric field spectra	<b>Plasma wave Electric spectra</b> for thermal-noise spectroscopy; sensitivity: 3 nV/ Hz; frequency range: 10-800 kHz. <b>Electric and magnetic spectra</b> and waveforms in an internal burst mode (triggered internally or on input), frequency range: near DC to 1 MHz	
<b>Remote Radio Waves</b>		<b>Radio waves</b> , 3-axis electric and magnetic spectra and correlations; frequency range: 100 kHz to 20 MHz	Wider frequency range – link to ground-based measurements
<b>Photospheric Magnetic Fields</b>	<b>High-Res Mode:</b> Longitudinal magnetic field with accuracy of 0.1 G (longitudinal); Pixel size: 1 arcsec, Cadence: 2 min over selected periods of time; Field of view: $> 15\text{ arcmin}$ <b>Low-Res. (full disk) Mode:</b> (a) Longitudinal magnetic field with accuracy of 0.1 G (longitudinal) (TBC) Pixel size: $\sim 5\text{ arcsec}$ ; Capability: cadence of 2 min over selected period of times on the whole orbit Cadence: synoptic measurements at least once every six hours FOV: $> 150\text{ arcmin}$ (full apparent Sun) (b) Continuum imaging, capability for Doppler measurements on the whole orbit, cadence of 1 min (resolution can be reduced) out of perihelion passage	<b>High-Res Mode:</b> Vector magnetic field with accuracy of 0.1 G (longitudinal), 2 G (transverse); Pixel size: 0.5 arcsec, Cadence: 1 min over selected periods of time; Field of view: $> 15\text{ arcmin}$ <b>Low-Res. (full disk) Mode:</b> (a) Vector magnetic field with accuracy of 0.1 G (longitudinal), 2 G (transverse); Pixel size: $\sim 5\text{ arcsec}$ ; Capability: Cadence of 1 min. over selected period of times on the whole orbit Cadence: synoptic measurements at least once every six hours FOV: $> 150\text{ arcmin}$ (full apparent Sun) (b) Continuum imaging, Doppler measurements on the whole orbit, cadence of 1 min	High data rate

Table 3.2 (cont'd) Solar Orbital Measurement Requirements			
Objectives	Minimum Measurements	Baseline Measurements	Augmented Measurements
<b>EUV Spectroscopy</b>	<b>On disk:</b> <ul style="list-style-type: none"> <li>- Best spatial resolution 2 arcsec</li> <li>- Instantaneous FOV = 8 arcmin x 2arcsec - Rastered FOV = 8 arcmin x 4 arcmin</li> <li>- One line per temperature decade</li> <li>- One spectral line per temperature decade (<math>10^4</math>-<math>10^7</math> K)</li> <li>- Exposure time 20 s</li> <li>- Compositional signatures</li> <li>- Spectral cadence of 40 min</li> </ul> <b>Off disk:</b> <ul style="list-style-type: none"> <li>- Best spatial resolution 2 arcmin</li> <li>- Stare (no raster)</li> <li>- Spectral cadence of 20 min</li> <li>- Compositional signatures and outflow</li> </ul>	<b>On disk:</b> <ul style="list-style-type: none"> <li>- Best spatial resolution 1 arcsec</li> <li>- IFOV = 16 arcmin x 1 arcsec</li> <li>- RFOV = 16 arcmin x 4 arcmin</li> <li>- Two lines per temperature decade</li> <li>- Exposure time 5 s</li> <li>- Spectral cadence of 20 min</li> <li>- Compositional signatures</li> </ul> <b>Off disk:</b> <ul style="list-style-type: none"> <li>- Spatial resolution 1 arcmin</li> <li>- Stare (no raster)</li> <li>- Spectral cadence of 10 min</li> <li>- Radial coverage out to 2 <math>R_s</math></li> <li>- Compositional signatures and outflow</li> </ul>	Additional data rate for on disk observation of CMEs and transients
<b>EUV Imaging</b>	<b>(a) FSI:</b> 1 passband (cool/hot TBD), 4° FOV, 2k format (7.2 arcsec/pixel), 2 min maximum cadence, SNR>2 in QS (dimmings) and off limb (CME ejecta). <b>(b) HRI:</b> 1 passband, 17 arcmin FOV, > 1k format, 10 s cadence in burst mode, SNR>3 on AR loops (nanoflares).	<b>(a) FSI:</b> 2 passbands (cool/hot TBD), 5.5° FOV, 7.2 arcsec/pixel, 1 min maximum cadence, SNR>2 in QS (dimmings) and off limb (CME ejecta). <b>(b) HRI:</b> 2 passbands, 17 arcmin FOV, >1k format, 5 s cadence in burst mode, SNR>5 on AR loops (nanoflares).	<b>(a) FSI:</b> 3 or more passbands (cool/hot TBD, and/or LOS Doppler measurement), 5.5° FOV, >2k format, 1 min maximum cadence, SNR>2 in QS (dimmings) and off limb (CME ejecta). <b>(b) HRI:</b> 3 or more passbands (same as FSI - TBC), 17 arcmin FOV, >1k format, <1 s cadence in burst mode, SNR>5 on AR loops (nanoflares).
<b>Near-Sun Coronagraphy</b>	<u>Polarized visible-light (VL) imaging:</u> Physical quantity: electron density FOV: ~1.2 to 3.5 $R_\odot$ . (at 0.23 AU) ; 3 - 15 $R_\odot$ (at 1 AU) Spatial res:< 8 arcsec ( $10^3$ km at 0.23 AU) Spectral coverage: 450-650 nm Stray-light rejection: $10^{-11}$ B/B $_\odot$ Polarization S/N: > $10^2$ Cadence: 5 min. (CMEs obs.); 10 min. (synoptic)	<u>Polarized visible-light imaging:</u> As for minimum observations <u>UV &amp; EUV imaging:</u> Physical quantities: hydrogen and singly-ionized helium densities, and outflow velocities FOV: ~1.2 to 3.5 $R_\odot$ . (SoIo at 0.23 AU) Extendable to 3 - 15 $R_\odot$ (SoIo at 1 AU) Spatial resolution: < 8 arcsec Spectral coverage: HI Ly- $\alpha$ , 121.6 nm; HeII Ly- $\alpha$ , 30.4 nm Spectral Resolution: $\lambda/\lambda \leq 10^{-1}$ Cadence: < 15 min.	<u>Polarized visible-light imaging:</u> As for minimum observations <u>UV/EUV spectroscopy &amp; imaging:</u> Physical quantities: hydrogen and singly-ionized helium densities, outflow velocities and kinetic distributions. FOV: ~1.2 to 3.5 $R_\odot$ . (at 0.23 AU). Extendable to 3 - 15 $R_\odot$ (at 1 AU) Spectral coverage: HI Lyman- $\alpha$ , 121.6 nm; HeII Lyman- $\alpha$ , 30.4 nm Spectral Resolution: $\lambda/\lambda \leq 10^{-4}$ Minimum most probable ( $e^{-1}$ ) speed and line-of-sight velocity: H $^0$ 30 km/s; He $^+$ 120 km/s; S/N: > 10 (line profile); > $10^2$ (integrated profile); Cadence: < 20 min.
<b>Wide-FOV Coronagraphy or Heliospheric Imaging (HI)</b>	<u>Visible-light (VL) imaging:</u> Physical quantity: electron distribution FOV: substantial coverage of the Sentinels orbit Spatial res: $\square$ arcmin Stray-light rejection: $10^{-14}$ B/B $_\odot$ Cadence: 2 hours	<u>Visible-light (VL) imaging:</u> Physical quantity: electron distribution FOV: substantial coverage of the Sentinels orbit Spatial res: $\square$ arcmin Stray-light rejection: $10^{-14}$ B/B $_\odot$ Cadence: 60 min.	<u>Polarized/bandpass visible-light imaging:</u> Physical quantity: electron density FOV: > substantial coverage of the Sentinels orbit Spatial res: $\square$ arcmin Stray-light rejection: $10^{-14}$ B/B $_\odot$ Cadence: 60 min.
<b>X-Ray Imaging and Spectroscopy</b>	Energy range: <~5 to >~50 keV, resolution $\square$ E/E <~0.4 FWHM, to cover thermal and non-thermal (accelerated electrons); Angular Resolution: <~10 arcsec; Angular FOV for imaging: >~15 arcmin; FOV for source centroid location: Full Sun at 0.222 AU, i.e. ~150 arcmin; Effective area >~5 cm $^2$ ; Time resolution (for flares) < ~10 s	Energy range: 3 to 150 keV; Energy resolution: $\square$ E/E ~0.2 FWHM; Angular Resolution: <~7 arcsec; FOV for imaging: >~20 arcmin; FOV for source centroid location: Full Sun at 0.222 AU, i.e. ~150 arcmin; Effective area ~ 15 cm $^2$ ; time resolution (for flares) <~5 s, ~1 s in Burst mode TBD	Baseline plus extended energy range: ~3 to 300 keV
Measurements to be performed on either Solar Orbiter or Sentinels only			
<b>Gamma-Ray Detection</b>	Energy range: ~0.4 to 8 MeV; energy resolution: $\square$ E/E <~0.1 at 1MeV; photopeak effective area >10 cm $^2$ at 1MeV; FOV: Full Sun; time resolution <~1 min, 20 s in flares	Energy range: ~0.3 to 10 MeV; energy resolution: E/E ~0.05; Field of view: Full Sun; Photopeak effective area at 1MeV > 20 cm $^2$ ; time resolution: normal ~20 s, with <~5 s in flares (Burst mode TBD)	Baseline plus extended energy range:~ 0.3 – 100 MeV; resolution E/E ~0.03
<b>Neutrons</b>	Energy range: ~1 to >~10 MeV; resolution: $\square$ E/E ~0.4; Field of view: Full Sun; time resolution: Normal cadence ~1 min, with burst mode TBD (during flares)	Energy range: ~1 to ~100 MeV; resolution: $\square$ E/E ~0.2; Field of view: Full Sun; time resolution: Normal cadence ~20 s, with burst mode TBD (during flares)	Baseline plus <~30° angular resolution to reject non-solar (s/c produced) background

Table 3-4. Prioritized Sentinels Measurements			
Objectives	Minimum Measurements	Baseline Measurements	Augmented Measurements
<b>Energetic Electrons</b>	Energy range: ~2 keV to ~5 MeV, energy resolution: $\Delta E/E \sim 0.2$ , angular resolution $\sim 30^\circ$ over a wide FOV as close to Sun as possible, covering $\sim 360^\circ$ in azimuth; geometric factor $> \sim 0.1\text{-}1\text{ cm}^2\text{sr}$ ; time resolution 10s at $< 0.5\text{ AU}$ , 1 min $> 0.5\text{ AU}$	Same as minimum plus Burst mode TBD Energy range: ~2 keV to ~10 MeV	High angular resolution $\sim 3^\circ$
<b>Energetic Protons</b>	Energy range: 0.05 to 100 MeV; energy resolution: $\Delta E/E \sim 0.2$ ; angular resolution $30^\circ$ over a wide FOV as close to Sun as possible, covering $\sim 360^\circ$ in azimuth ; geometry factor $> \sim 0.1\text{-}1\text{ cm}^2\text{sr}$ ; time resolution 20s below 10 MeV at $< 0.5\text{ AU}$ , 1 min $> 0.5\text{ AU}$	Same as minimum plus Burst mode TBD, plus extended energy range 0.005 to 500 MeV	Higher angular resolution $\sim 3^\circ$ , closer to full 4 $\pi$ sky coverage
<b>Energetic Heavy Ions</b>	He – Fe, energy range: 0.02 – 30 MeV/nucleon (species dependent) Composition: separate $^3\text{He}$ , $^4\text{He}$ , C,N,O and Fe as a minimum; energy resolution: $\Delta E/E \sim 0.2$ ; angular resolution $30^\circ$ over a wide FOV as close to Sun as possible, covering $\sim 360^\circ$ in azimuth; geometry factor $> \sim 0.1\text{-}1\text{ cm}^2\text{sr}$ ; time resolution 30s $< 0.5\text{ AU}$ , 1min $> 0.5\text{ AU}$	Minimum plus energy range to 100 MeV/nucleon (species dependent); Burst mode TBD	Baseline plus extended energy range down to 0.005 MeV/nucleon, species up to ultra-heavy, $Z > 30$ .
<b>Energetic Particle Charge State</b>	Average charge states He to Fe, 10-300 keV/charge	Minimum plus Energy range $\sim 10\text{keV}$ to 1 MeV/charge, time resolution 15 min	Baseline plus individual charge states
<b>Solar Wind Ions</b>	Simple 1-dim energy spectra (0.2 – 20 keV/q, 5% resolution) of protons and alphas at low time resolution (1 minute), solar wind velocity, density and temperature	Detailed 3-dim velocity distribution functions at spin time-resolution; FOV: $\pm 45^\circ$ north/south, angular resolution of $2^\circ$	Burst mode at better than 1s time resolution to resolve kinetic effects
<b>Solar Wind Electrons</b>	Core electron density and temperature, electron strahl pitch angle distribution at $\sim 50\text{eV}$ and above; 1 minute	3-dim velocity distribution functions (1 -2000 eV, 10% energy resolution); FOV: $\pm 45^\circ$ north/south, angular resolution $10^\circ$ , core-halo electron pitch-angle distributions with strahl population; spin resolution	Burst mode: The microphysics of electrons (whistler-electron interactions) can be measured with the radio wave analyzer.
<b>Solar Wind Composition</b>	Selected heavy ions (C, N, O and Fe) for abundances and charge states; 10 minutes at 0.25 AU	Many heavy ion 1-dim energy spectra (0.5 – 60 keV/q, 5% energy resolution); FOV like for protons; temperature anisotropy and differential speed; cadence: 1 min.	
<b>DC Vector Magnetic Fields</b>	$\pm 1000\text{ nT}$ , 1 minute time resolution; 1nT absolute precision	$\pm 1000\text{ nT}$ , 0.5nT absolute precision; 0-20 Hz; time resolution 3 s	Burst mode to 100Hz for shock waves
<b>AC Magnetic Fields</b>		10Hz – 10kHz; waveform capture; cadence for spectra	Enhanced burst mode capture
<b>Local Plasma Waves</b>	On Solar Orbiter	On Solar Orbiter	<b>Electric spectra</b> for thermal-noise spectroscopy; sensitivity: 3 nV/ Hz; frequency range: 10-800 kHz. <b>Electric and magnetic spectra</b> and waveforms in an internal burst mode (triggered internally or on input), frequency range: near DC to 1 MHz.
<b>Remote Radio Waves</b>	<b>Radio waves</b> , 2-axis electric and magnetic spectra and correlations; frequency range: 100 kHz to 20 MHz.	<b>Radio waves</b> , 3-axis electric and magnetic spectra and correlations; frequency range: 100 kHz to 20 MHz.	Wider frequency range – link to ground-based measurements
<b>X-ray imaging and spectroscopy</b>	X-ray imaging & spectroscopy on Solar Orbiter	Energy range: $< \sim 5$ to $> \sim 40\text{ keV}$ for imaging; Energy resolution $\Delta E/E < \sim 0.4$ FWHM; Angular Resolution: $< \sim 30\text{ arcsec}$ ; Angular FOV for imaging: full Sun; Effective area $> \sim 5\text{ cm}^2$ ( $\sim 20\%$ duty cycle); Time resolution (for flares) $< \sim 10\text{ sec}$	Energy range: $\sim 4$ to 80 keV for imaging; Energy resolution: $\Delta E/E \sim 0.2$ FWHM; Angular Resolution: $< \sim 20\text{ arcsec}$ ; FOV for imaging: full Sun; Effective area $> \sim 10\text{ cm}^2$ ( $\sim 20\%$ duty cycle); Time resolution (for flares) one spin (Burst mode)
<b>EUV Imaging</b>			<b>Full Sun Imager (FSI)</b> on 2 to 4 IHS: 1 passband (cool/hot TBD), $5^\circ$ FOV, $> 64 \times 64$ format, 10 min cadence, SNR $>2$ in QS (dimmings)
Measurements to be performed on either Solar Orbiter or Sentinels only			
<b>Gamma-Ray</b>	Energy range: $\sim 0.4$ to 8 MeV; energy resolution: $\Delta E/E < \sim 0.1$ @ 1MeV; photopeak effective area $> 10\text{ cm}^2$ @ 1MeV; FOV: Full Sun; time resolution $< \sim 1\text{ min}$ , 20s in flares	Energy range: $\sim 0.3$ to 10 MeV; energy resolution: $\Delta E/E \sim 0.05$ ; Field of view: Full Sun; Photopeak effective area @ 1MeV $> 20\text{ cm}^2$ ; time resolution: normal $\sim 20\text{ s}$ , with $< \sim 5\text{ s}$ in flares (Burst mode TBD)	Baseline plus extended energy range: $\sim 0.3$ – 100 MeV; resolution $\Delta E/E \sim 0.03$ @ 1MeV;
<b>Neutrons</b>	Energy range: $\sim 1$ to $\sim 10\text{ MeV}$ ; resolution: $\Delta E/E \sim 0.2$ ; Field of view: Full Sun; time resolution: Normal cadence $\sim 20\text{ s}$ , with TBD burst mode (during flares)	resolution: $\Delta E/E \sim 0.2$ ; Field of view: Full Sun; time resolution: Normal cadence $\sim 20\text{ s}$ , with burst mode (during flares)	

<b>Table 5-1. HELEX timeline for 2017 Sentinels launch</b>	
<b>Event</b>	<b>Date</b>
Solo Launch	2015 May 19
Solo VGA 1	2015 Nov 27
Solo EGA 1	2016 Oct 8
Sentinels Launch	2017 Mar 29
Sentinels 1,2,3,4 VGA 1	2017 Sept 16
Sentinels 1,2,4 VGA 2	2018 Apr 29
Sentinels 3 VGA 2	2018 Jul 8
Sentinels 1 1 <sup>st</sup> time below 0.5 AU	2018 Jul 13
Solo EGA 2	2018 Aug 8
Solo VGA 2	2018 Oct 10
Sentinels 4 VGA 3	2018 Dec 9
Solo at Min perihelion of 0.215 AU	2019 Apr 17
Sentinels 1 VGA 3	2019 Jul 22
Sentinels 2 VGA 3	2019 Aug 21
Sentinels 1 1 <sup>st</sup> Min perihelion @ 0.25 AU	2019 Sept 26
Sentinels 3 VGA 3	2019 Sept 30
Solo VGA 3	2020 Jan 3
Sentinels 4 VGA 4	2020 Mar 3
End of Sentinels Primary mission	2020 Mar 29
Solo VGA 4	2021 Mar 27
End of Solo Primary mission	2021 Jul 8
Solo at Max latitude of 34 degrees	2025 Mar 12

Yellow shading indicates time between the beginning of Solo science phase and end of Sentinels primary mission.